

Supporting information for SI-PET-RAFT in Flow: Improved Control over Polymer Brush Growth.

Andriy R. Kuzmyn,^{1*} Martijn van Galen,^{1,2,3} Barend van Lagen,¹ and Han Zuilhof^{1,4*}

1) Laboratory of Organic Chemistry, Wageningen University & Research, Stippeneng 4, 6708 WE Wageningen, The Netherlands. 2) Physical Chemistry and Soft Matter, Wageningen University & Research, Stippeneng 4, 6708 WE Wageningen, The Netherlands. 3) Laboratory of Biochemistry, Wageningen University and Research, Stippeneng 4, 6708 WE, Wageningen, the Netherlands 4) School of Pharmaceutical Sciences and Technology, Tianjin University, 92 Weijin Road, Tianjin, 300072, China.

Table of content

Materials and methods	S3
XPS characterization	S7
Kinetics measurements	S26
SMFS measurements	S30
References	S29

Corresponding authors

andrii.kuzmyn@wur.nl

han.zuilhof@wur.nl

Materials and methods

Materials. All chemical reagents were used without further purification unless otherwise specified. 4-Cyano-4-(phenylcarbonothioylthio)pentanoic acid N-succinimidyl ester (RAFT-NHS), 4-cyano-4-(phenylcarbonothioylthio)pentanoic acid, cysteamine, triethanolamine (TEOA), eosin Y (EY), erythrosin B (EB), phloxine B (Ph), Rose bengal (R), triethylamine (TEA), oligo(ethylene glycol) methyl ether methacrylate (average Mn 300) (MeOEGMA), ethanol (EtOH) (99.9%), acetone (99.5%), and dry tetrahydrofuran (THF, 99.9%) were purchased from Sigma-Aldrich. *N*-(2-Hydroxypropyl) methacrylamide (HPMA) was obtained from Polysciences. Inc. Deionized water was produced with a Milli-Q integral 3 system Millipore, Molsheim, France (Milli-Q water).

Light Source. LEDs with a maximum intensity at 410 nm (Intelligent LED Solutions, product number: ILH-X001-S410-SC211-WIR200) were used, and the current was set at 700 mA, corresponding to a total radiometric power of 2.9 W, according to manufacturer specifications. The light intensity of the halogen lamp was measured to be $3.5 \mu\text{W}\cdot\text{cm}^{-2}$.

Formation of RAFT agent-functionalized monolayers. The RAFT-agent immobilization was conducted in accordance with previously published procedures.¹ The substrates were rinsed with, acetone, absolute ethanol (EtOH), and Milli-Q water, and blown dry under a gentle stream of Ar. Subsequently, the surfaces were exposed to an oxygen plasma for 5 min in a plasma cleaner (100 W; 5 mbar O₂; Diener electronic GmbH, Germany). The freshly activated surfaces were immediately immersed in a freshly prepared solution of (3-aminopropyl)triethoxysilane (APTES) ($1 \text{ mg}\cdot\text{mL}^{-1}$) in absolute ethanol at RT for 16 h. The substrates were subsequently rinsed with EtOH and Milli-Q water and blow-dried with Ar. After immobilization of the APTES on surfaces the substrates were submerged in a solution of RAFT-NHS (20 mg, 53 μmol) and TEA (7 mg, 10 μL , 72 μmol) in 1 mL of dry THF at RT for 16 h. The substrates were subsequently rinsed with THF, acetone, EtOH, and Milli-Q water and blow-dried with Ar. The substrates were stored under Ar protection before use.

SI-PET-RAFT synthesis of polymer brushes. The polymerization was conducted according to a modification of a previously reported procedure.¹ A dye stock solution with photocatalyst was prepared to contain: photocatalyst (39 μmol)(Table S1) and TEOA (160 mg, 1.60 mmol) in 10 mL of Milli-Q water.

Table S1. Concentration of different photocatalysts in the stock solution.

Photocatalyst	M _w	mg in on 10 mL
Eosin Y (EY)	647.89	25
Phloxine B (Ph)	829.63	32
Rose Bengal (R)	1017.64	40
Erythrosine B (EB)	835.89	33

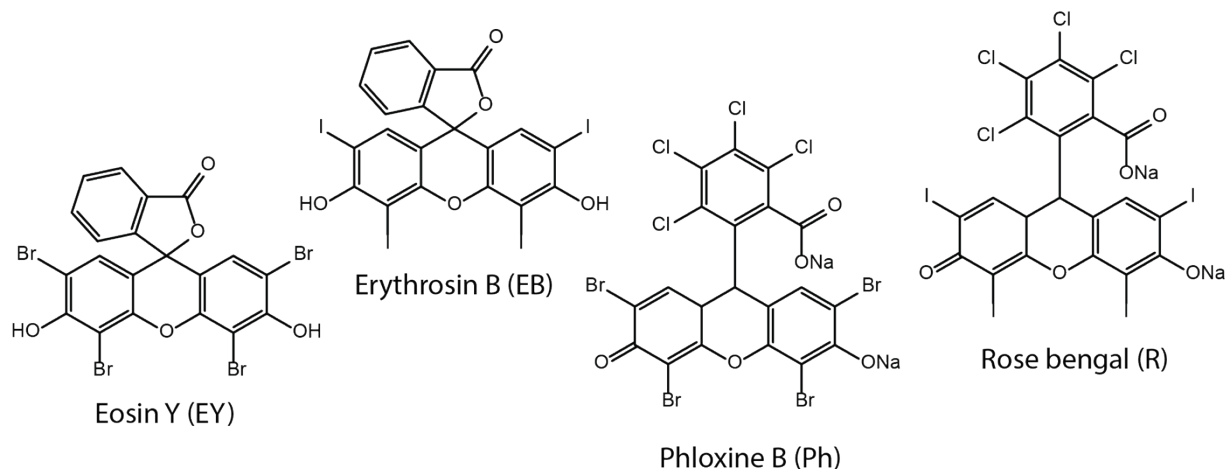


Figure S1. Chemical structures of the photocatalysts under current study.

The monomer MeOEGMA (94 mg, 0.30 mmol), was dissolved in Milli-Q water (1 mL), and subsequently, 10 μL of the stock solution was added. The mixture was vortexed and added to vials containing surfaces with an immobilized RAFT agent so that the liquid formed a thin layer (ca. 2 mm) on top of the surfaces. Immediately after this, the polymerization was conducted by irradiating the vials with visible light from a LED light source for different periods of time. In these experiments, the light source was placed 3–4 cm from the substrates. The polymerization was stopped by switching off the light source. The samples were then removed from the solution and subsequently rinsed with Milli-Q water, ethanol, and blown dry under a stream of argon.

In the case of the experiments in continuous flow conditions, the same polymerization solution composition was used but pumped with a continuous flow of $30 \text{ uL}\cdot\text{min}^{-1}$ and irradiated with 410 nm light. The flow-in setup consists of two glass slides. The upper glass slide has two luer-lock inlets for in and out of the polymerization solution. The bottom slide has curved channels for the liquid flow, and in the middle, there is a rectangular chamber. The sample with immobilized RAFT agent is immobilized in the rectangular chamber. The polymerization liquid is pumped using a syringe pump over the surfaces under irradiation.

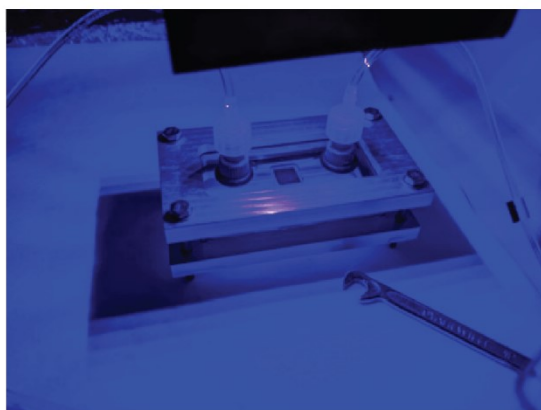
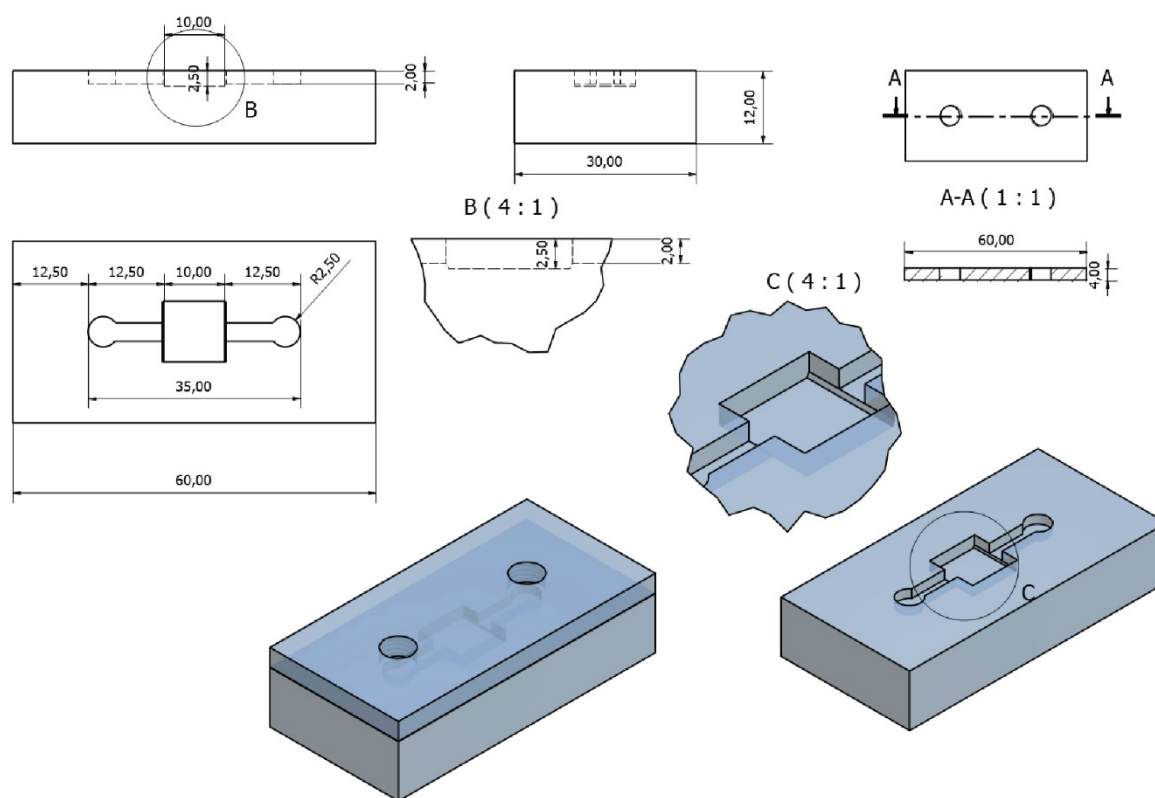


Figure S2. Photo SI-PET-RAFT reactor.

Patterned layers. The diblock copolymer was synthesized using solutions for the first block solutions MeOEGMA (94 mg, 0.30 mmol) second block solution HPMA (200 mg, 1.3 mmol) dissolved in Milli-Q water (1 mL) and subsequently added 10 μ L of the dye stock solution. The first solution was pumped through the flow chamber then samples were washed with water and ethanol dried. Following, the aluminum foil mask was attached to the flow reactor, and pumping of the second polymerization solution continued for 2 h under irradiation. The surfaces were removed from the solution and subsequently rinsed with Milli-Q water, and ethanol, and blown dry under a stream of argon.

X-ray photoelectron spectroscopy (XPS). XPS measurements were performed using a JPS-9200 photoelectron spectrometer (JEOL Ltd., Japan). All samples were analyzed using a focused monochromated Al K α X-ray source (spot size of 300 μ m) at a constant dwelling time for wide-scan 50 ms and narrow-scan of 100 ms and pass energy: wide-scan 50 eV narrow-scan: 10 eV. The power of the X-ray source was 240 W (20 mA and 12 kV). Charge compensation was applied during the XPS scans with an accelerating voltage of 2.8 eV. A filament current of 4.8 A. XPS wide-scan and narrow-scan spectra were obtained under ultra-high vacuum conditions (base pressure $3 \cdot 10^{-7}$ Pa). All narrow-range spectra were corrected with a linear background before fitting. The spectra were fitted with symmetrical Gaussian/Lorentzian (GL(30)) line shapes using CasaXPS. All spectra were referenced to the C1s peak attributed to C–C and C–H atoms at 285.0 eV.

The XPS mapping was performed utilizing a twin anode X-ray source was used at 15 kV and 10 mA with a resolution of $33 \times 33 \mu$ m per pixel.

Aminolysis. The chain-end RAFT-agent aminolysis was conducted in accordance with previously published procedures.² The solution containing 5 mL of anhydrous ethanol, hexylamine (20 μ L, 0.153 mmol) and TEA (20 μ L, 0.143 mmol) was deoxygenated by purging with argon for 15 min. Following the solutions were added in previously deoxygenated reactors containing substrates coated with poly(MeOEGMA) brushes. The reaction was allowed to proceed at room temperature for 3 h. Afterward, the substrates were washed with methanol, acetone, and twice with ethanol and DI water, then dried under a stream of Ar.

Spectroscopic ellipsometry. The polymerization kinetics were followed by measuring the dry thickness of the brushes using an Accurion Nanofilm_ep4 Imaging Ellipsometer. The ellipsometric data were acquired in the air at room temperature using light in the wavelength range of $\lambda = 410 - 810$ nm at an angle of incidence of 50°. The data were fitted with EP4 software using a multilayer model. Then, the polymer brush layers were described using a Cauchy model with parameters $A = 1.450 \pm 0.005$ and $B = 4500 \pm 100$.

Atomic force microscopy (AFM). AFM surface topography images were acquired by an Asylum Research MFP-3D Origin AFM (Oxford Instruments, United Kingdom). The instrument was operated in tapping mode and equipped with a silicon cantilever (AC240TS-R3, $k = 1.3$ N/m) with a nominal tip radius of ~ 7 nm. Gwyddion³ software was used to process and analyze the AFM topography images.

Single-molecule force spectroscopy (SMFS). The SMFS measurements were carried out in Milli-Q water. Force spectroscopy experiments were performed on a JPK ForceRobot® 300 automated force spectroscope working in contact mode in a fluid cell filled with gold-coated tips (MikroMasch, HQ:CSC38/Cr–Au, consisting of three cantilevers; cantilever B was used for measurements; with a nominal tip radius of 35 nm). After mounting the cantilever, sensitivity, and spring constant calibration was performed prior to the SMFS measurements. The average sensitivity and spring constant were determined to be 59.12 ± 8.83 nm·V⁻¹, 0.089 ± 0.015 N·m⁻¹. Between 6,000 – 20,000 force curves were measured for each sample in 3-4 different areas of the sample. The tip separation from the sample was 1000 nm. The data was processed by JPKSPM Data Processing, where the curves showing a clear unfolding and rupture event were selected. On average 1% of the recorded curves showed a single rupture event. These curves were further fitted to the worm-like chain (WLC)(S1) model to obtain the contour and persistence length. The molar mass of polymer brushes was calculated by dividing the average contour length by the size of repeat monomer unit (C–C–C bonds along the main chain, i.e., 0.273 nm) and multiplying on average M_n monomer unit 300.

Calculation of surface parameters of poly(MeOEMA) layers

Analysis of SMFS data using a worm-like chain model (WLC)

$$f(x) = \frac{K_b T}{L_p} \left(\frac{1}{4 \left(1 - \frac{x}{L_c}\right)} - \frac{1}{4} + \frac{x}{L_c} \right) \quad (S1)$$

where x is distance, $f(x)$ is pull-off force, K_b is Boltzmann constant, T is the absolute temperature, L_p persistence length, and L_c contour length.

The grafting density σ chain·nm⁻² of polymer brushes was determined by :

$$\sigma = \frac{h \rho N_A}{M_n} \quad (S2)$$

Using the ellipsometric thickness h , the bulk density of poly(MeOEGMA) was taken to be 1.05 g·cm⁻³, and N_A is the Avogadro constant.

Reduced grafting density (Σ)

$$\Sigma = \sigma \pi R_g^2 \quad (S3)$$

R_g is the radius of gyration (approximated to be $R_g \cong \sqrt{3} M_n$)

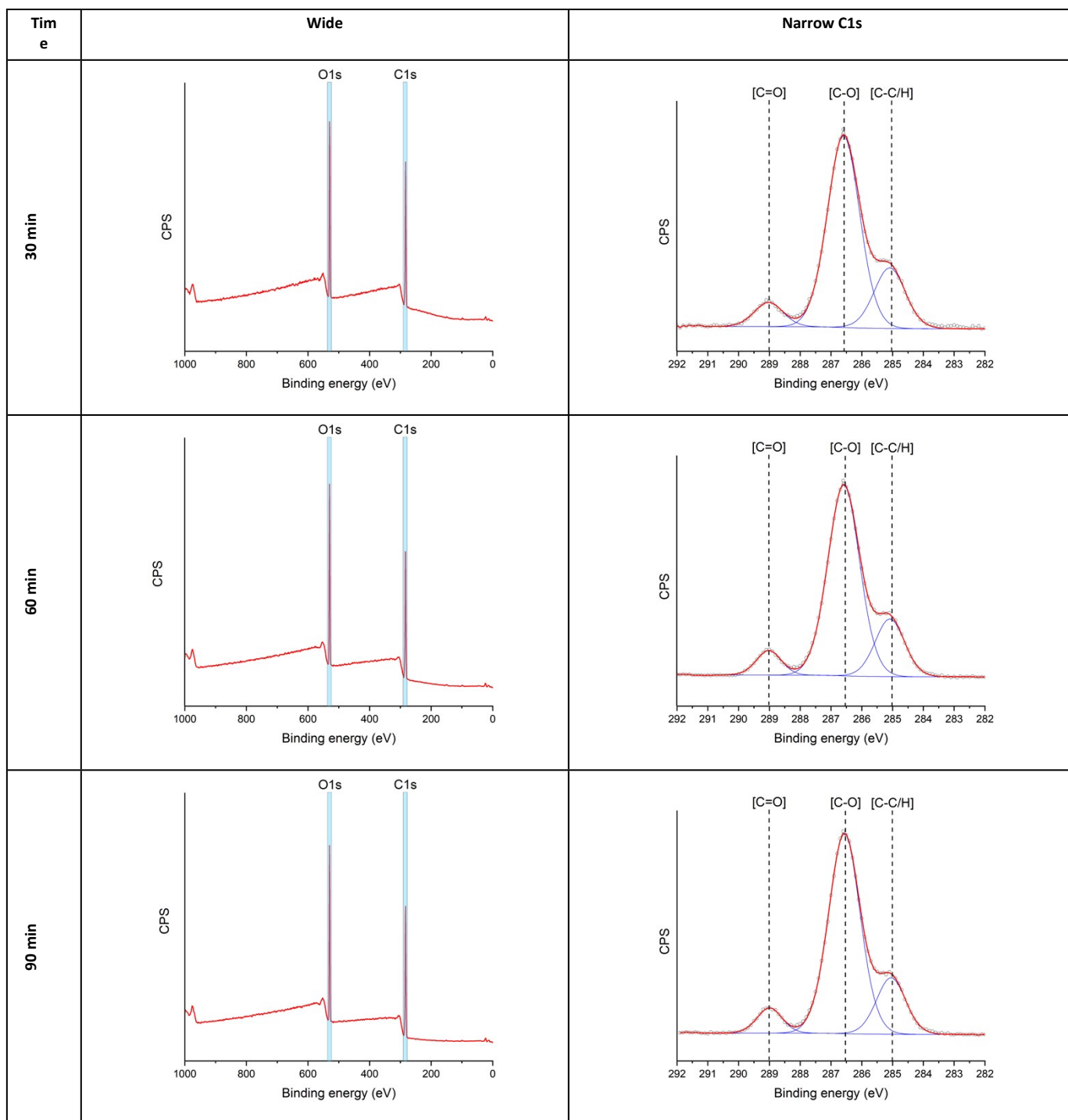
The relationship between M_n and dry thickness (h) was fitted using linear fit :

$$M_n = 5740 \cdot h + 91503 \text{ with } R^2 = 0.9506 \text{ in flow conditions (S4)}$$

$$M_n = 43541 \cdot h + 71829 \text{ with } R^2 = 0.8906 \text{ in no-flow conditions (S5)}$$

XPS characterization

Table S2. XPS characterization of poly(MeOEGMA) brushes obtained by SI-PET-RAFT in no-flow conditions, EY photocatalyst, wide and narrow C1s XPS spectra at different time points of polymerization.



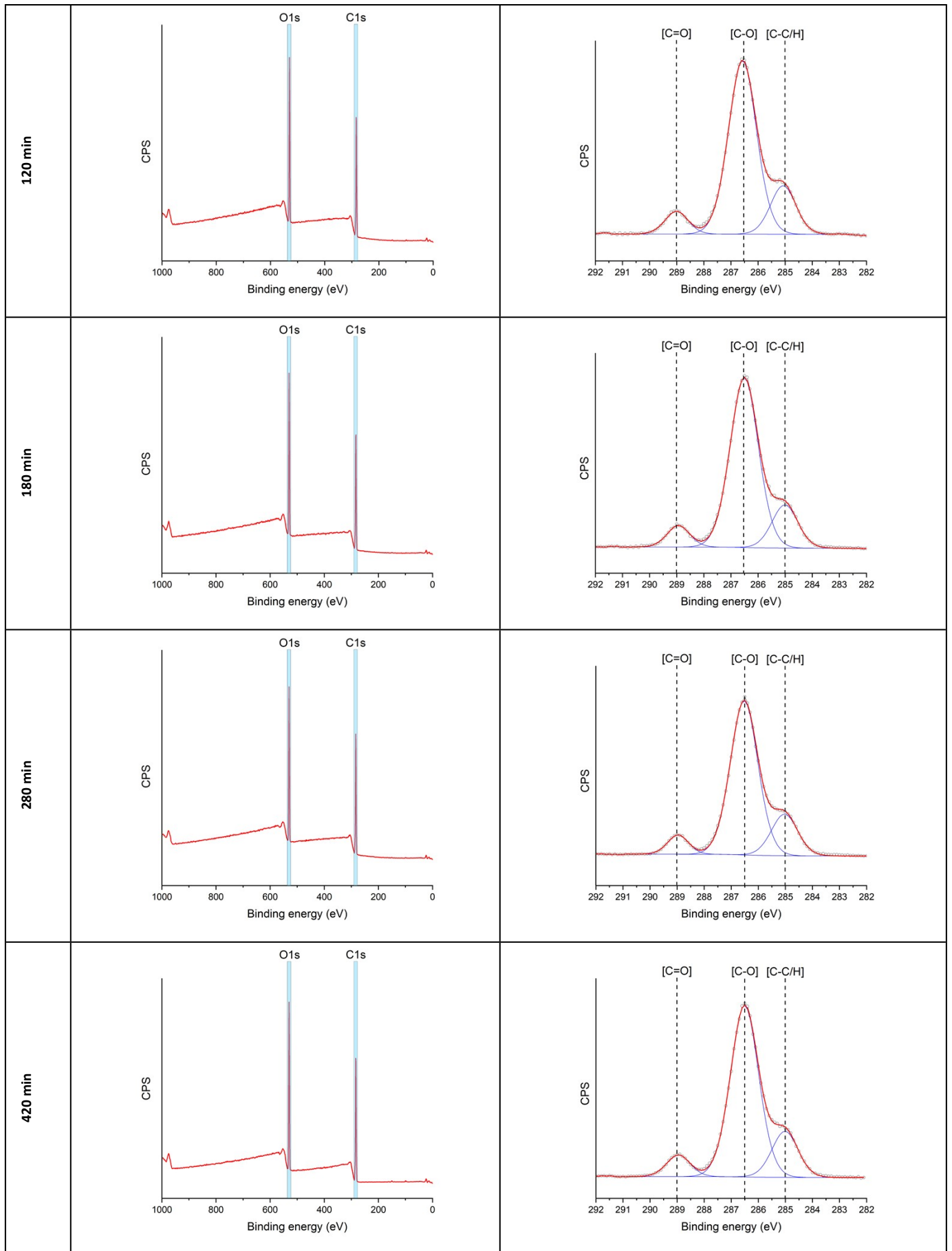
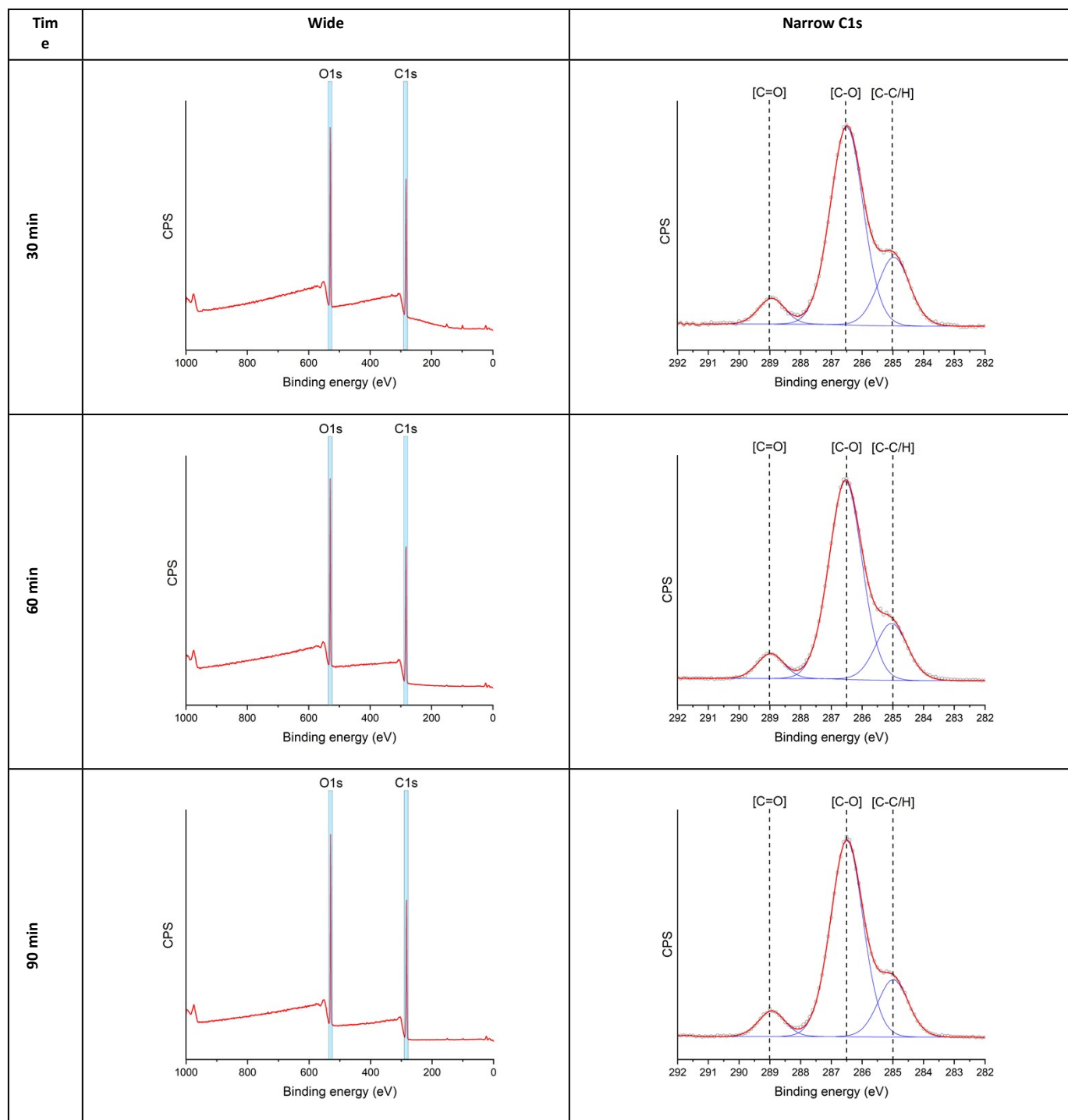


Table S3. XPS characterization of poly(MeOEGMA) brushes obtained by SI-PET-RAFT in flow conditions, EY photocatalyst, wide and narrow C1s XPS spectra at different time points of polymerization.



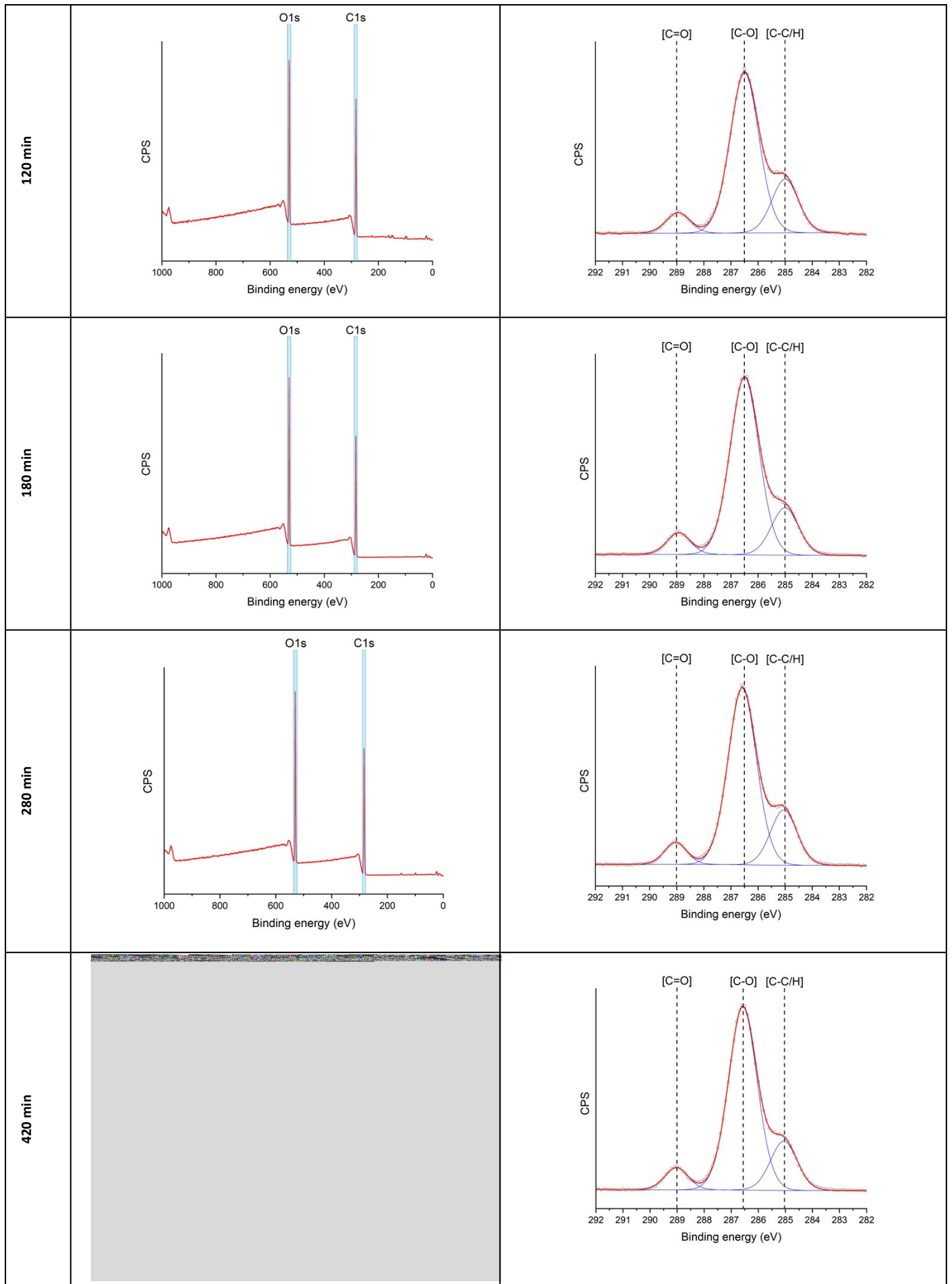
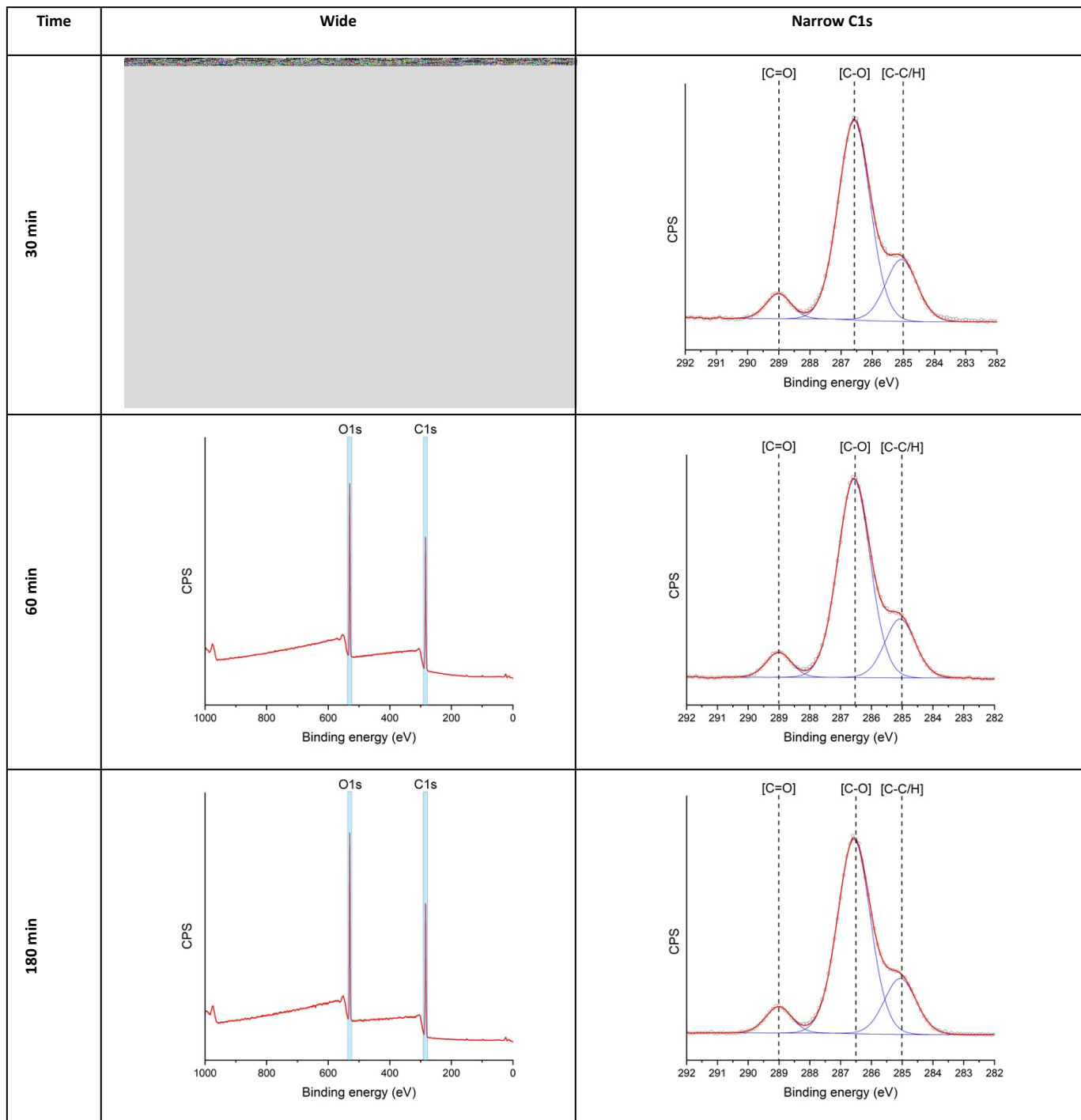


Table S4. XPS characterization of poly(MeOEGMA) brushes obtained by SI-PET-RAFT in no-flow conditions, R photocatalyst, wide and narrow C1s XPS spectra at different time points of polymerization.



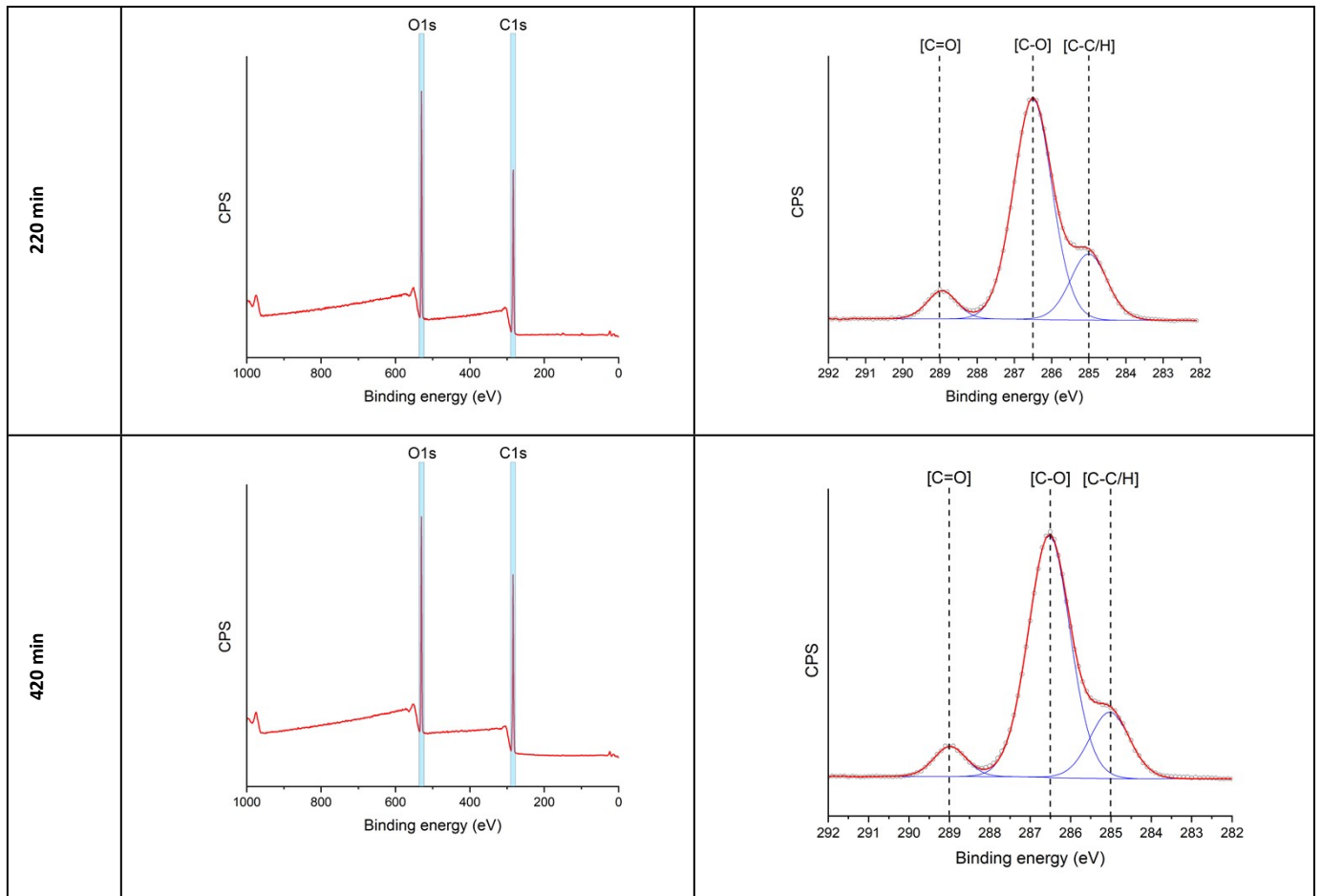
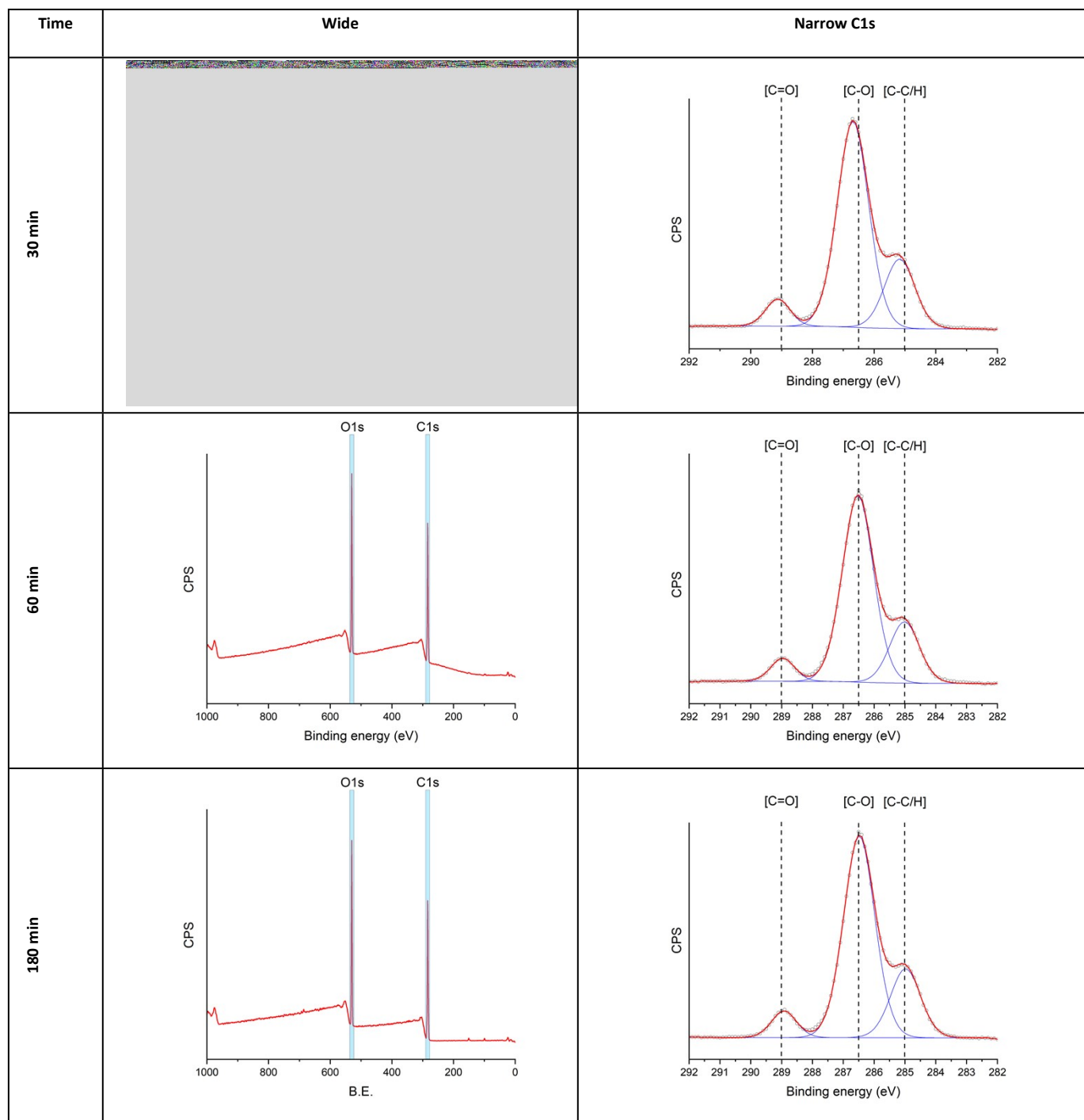


Table S5. XPS characterization of poly(MeOEGMA) brushes obtained by SI-PET-RAFT in flow conditions, R photocatalyst, wide and narrow C1s XPS spectra at different time points of polymerization.



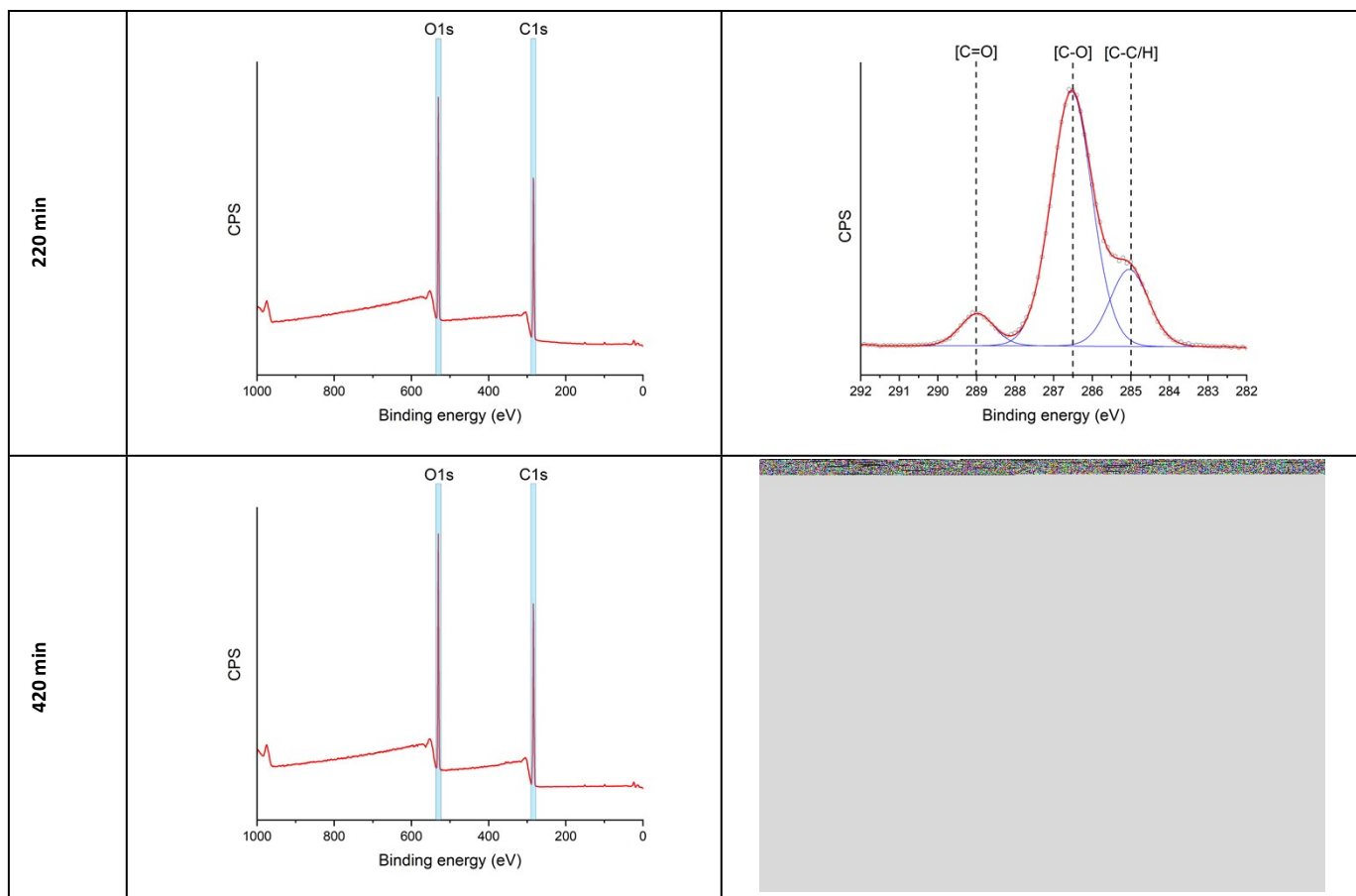
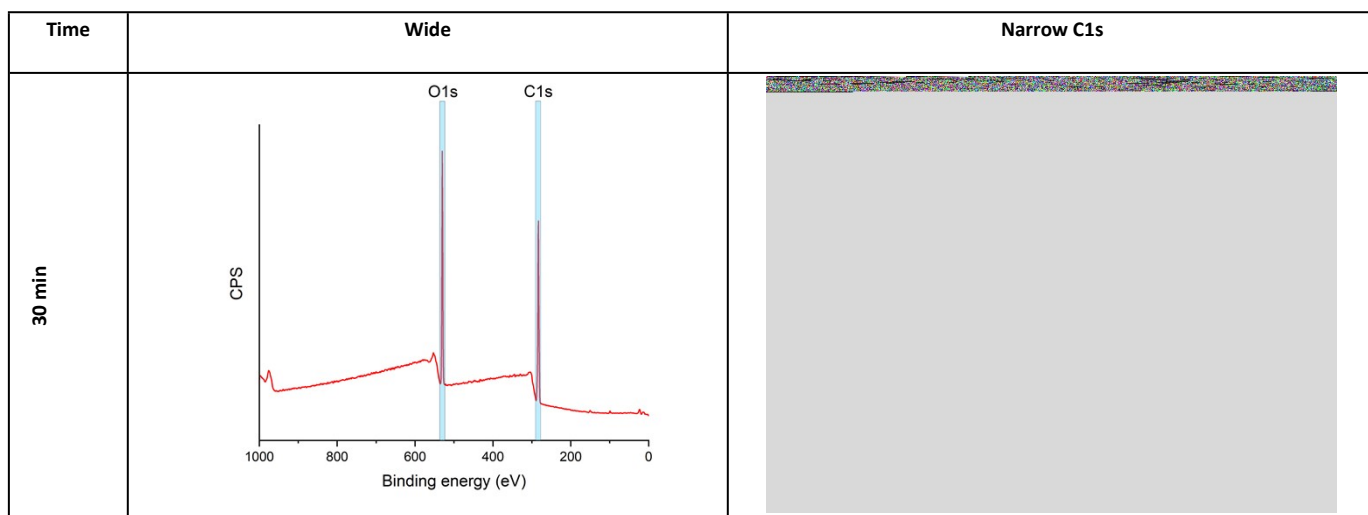
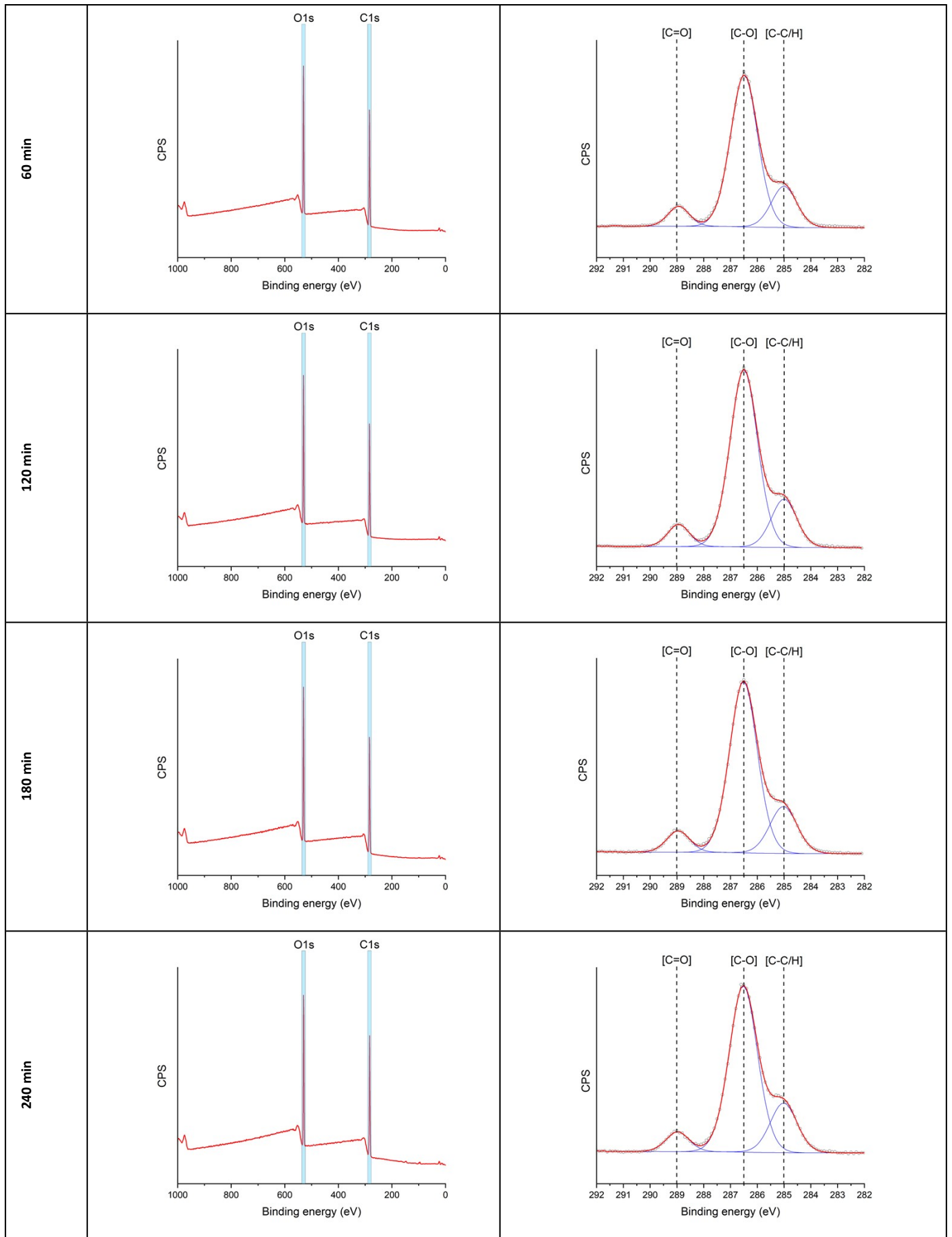


Table S6. XPS characterization of poly(MeOEGMA) brushes obtained by SI-PET-RAFT in no-flow conditions, Ph photocatalyst, wide and narrow C1s XPS spectra at different time points of polymerization.





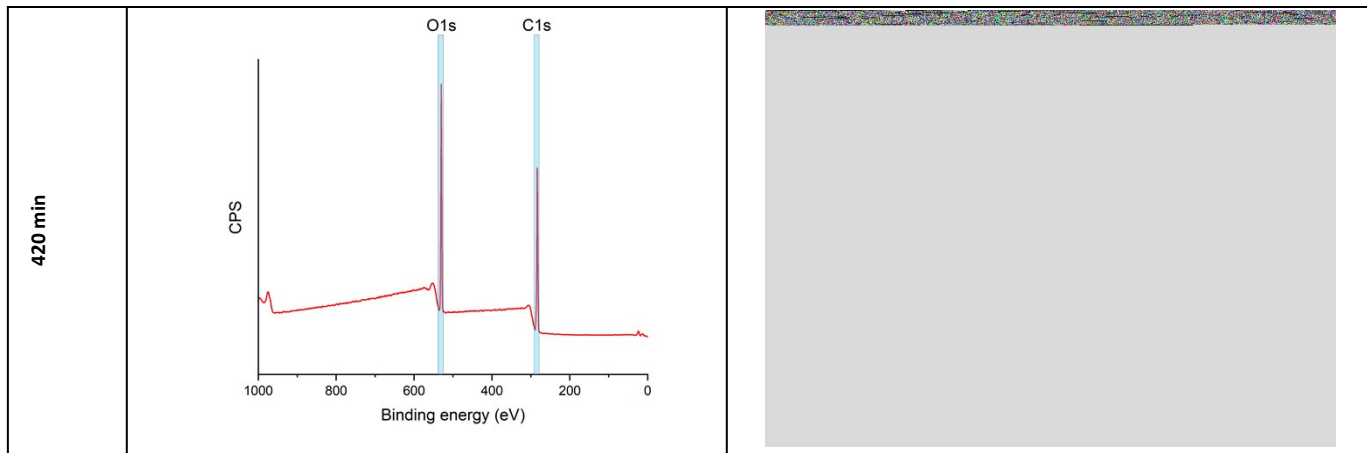
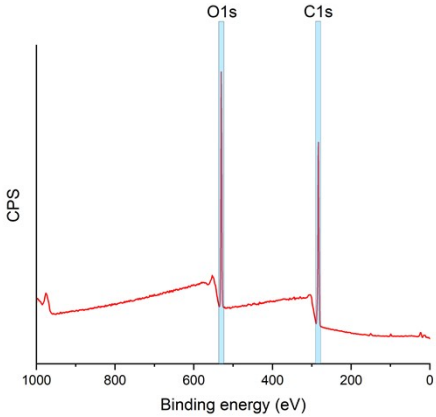
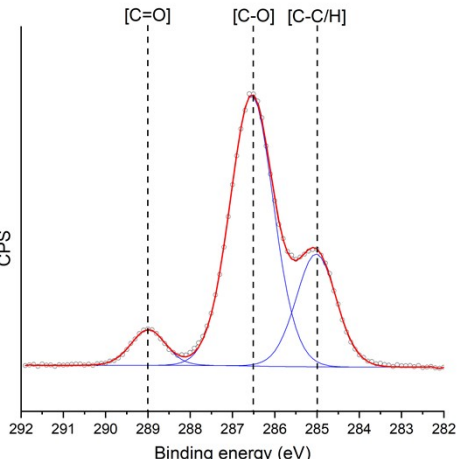
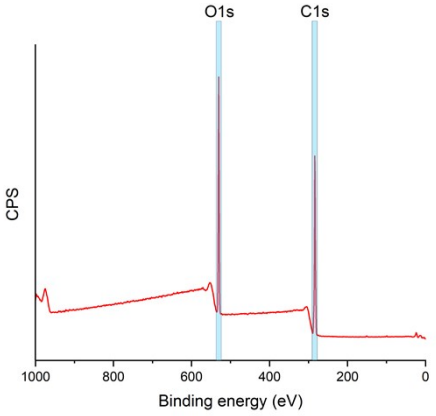
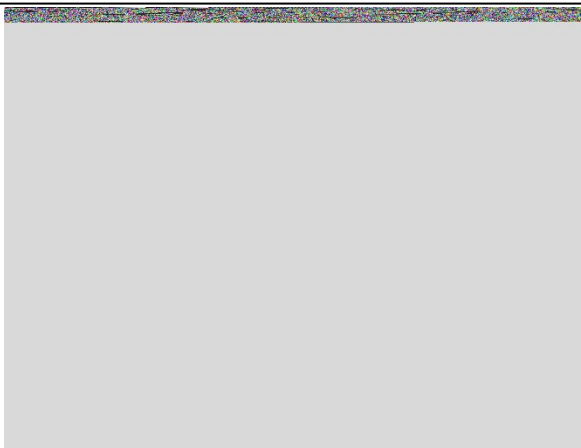
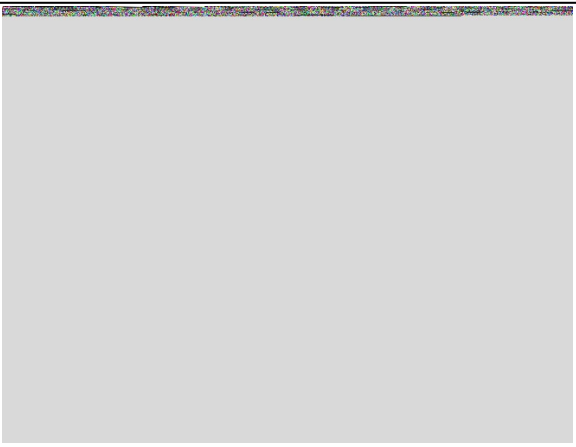
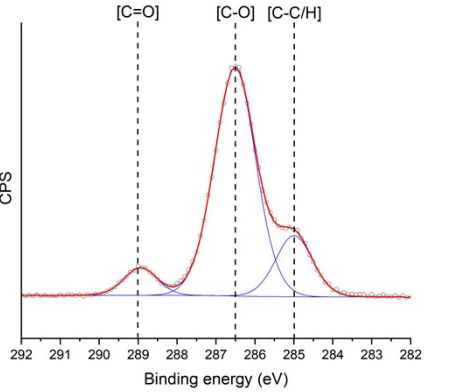


Table S7. XPS characterization of poly(MeOEGMA) brushes obtained by SI-PET-RAFT in flow conditions, Ph photocatalyst, wide and narrow C1s XPS spectra at different time points of polymerization.

Time	Wide	Narrow C1s
30 min		
60 min		
120 min		

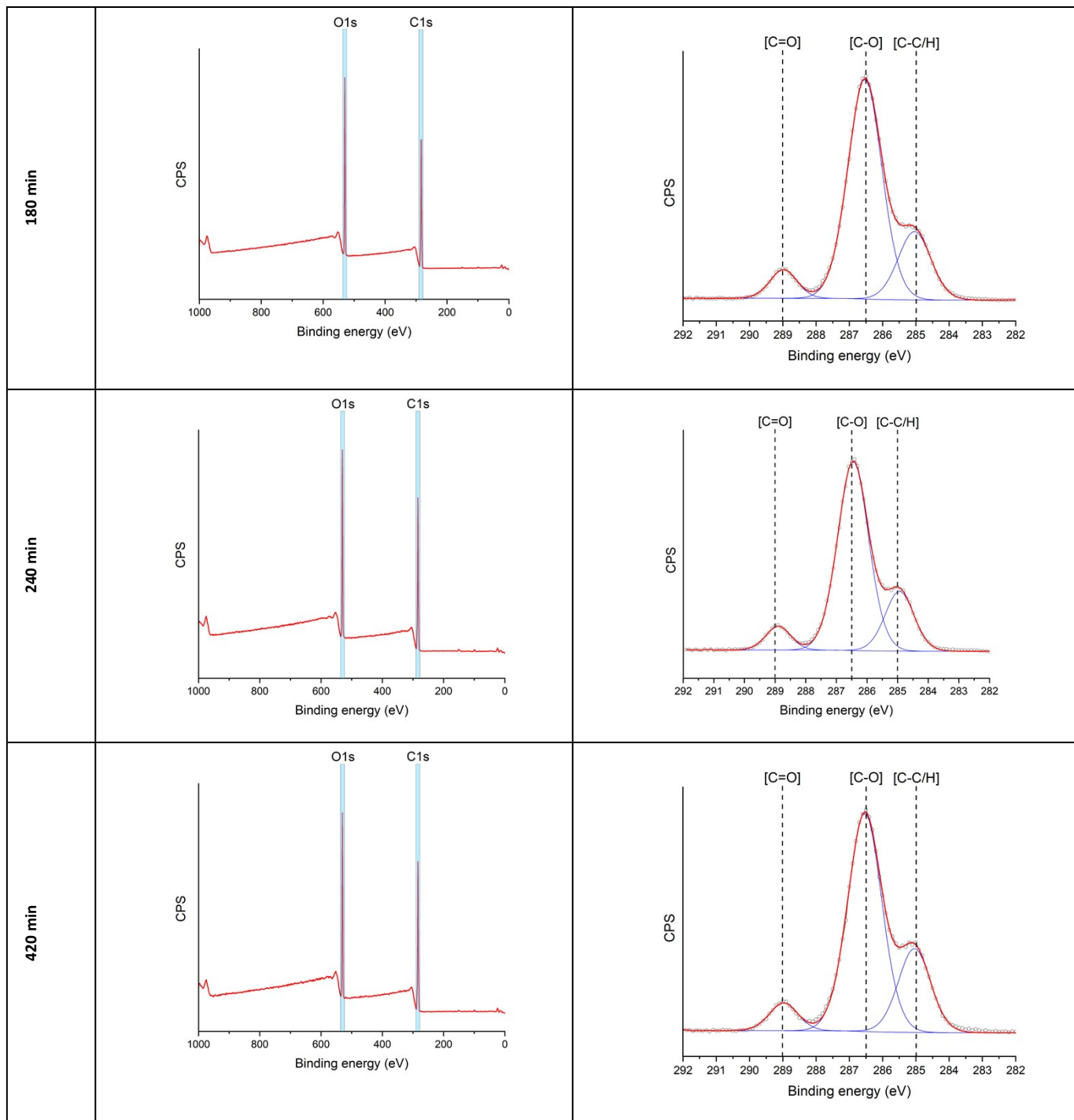


Table S8. XPS characterization of poly(MeOEGMA) brushes obtained by SI-PET-RAFT in no-flow conditions, EB photocatalyst, wide and narrow C1s XPS spectra at different time points of polymerization.

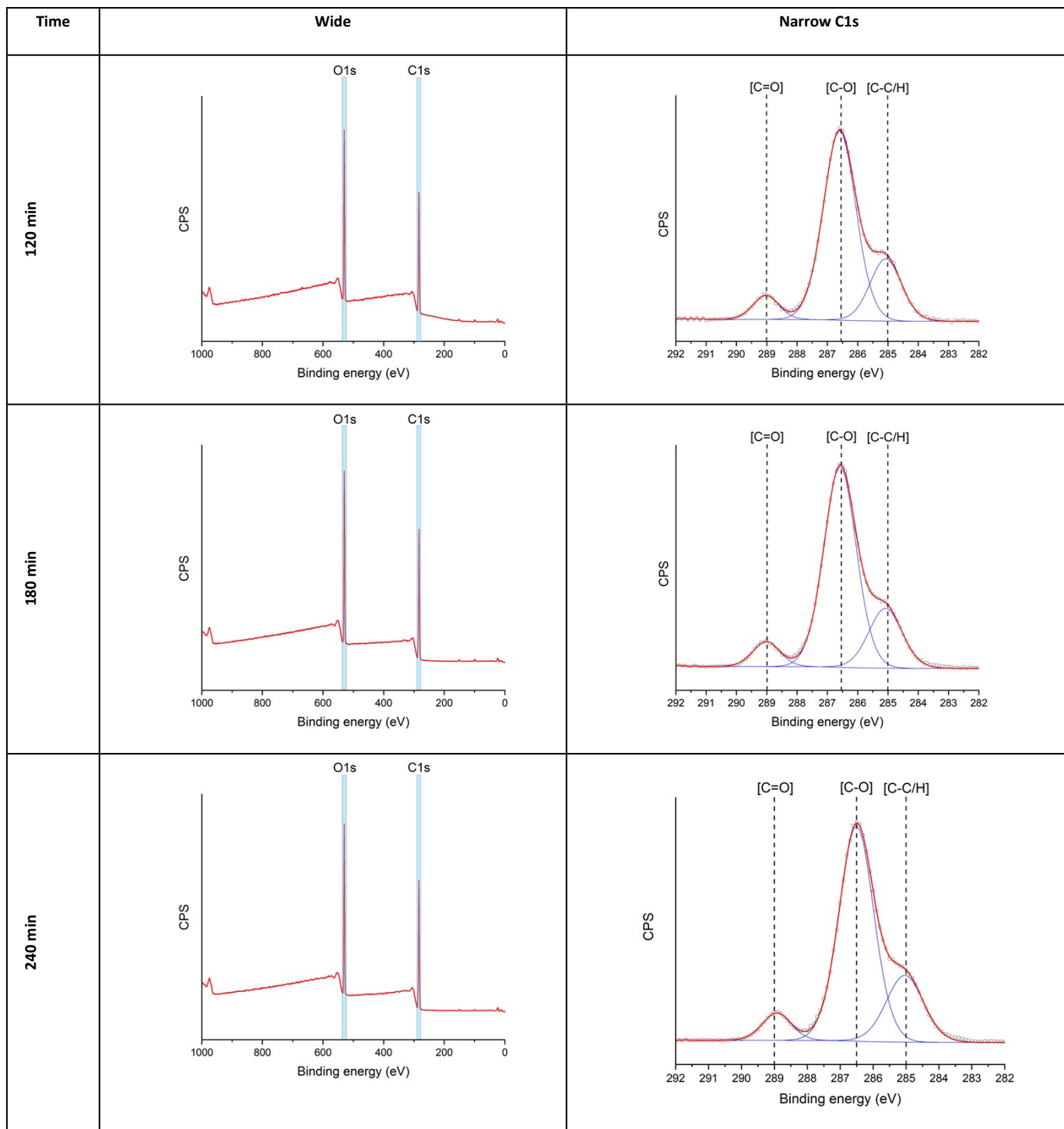


Table S9. XPS characterization of poly(MeOEGMA) brushes obtained by SI-PET-RAFT in flow conditions, EB photocatalyst, wide and narrow C1s XPS spectra at different time points of polymerization.

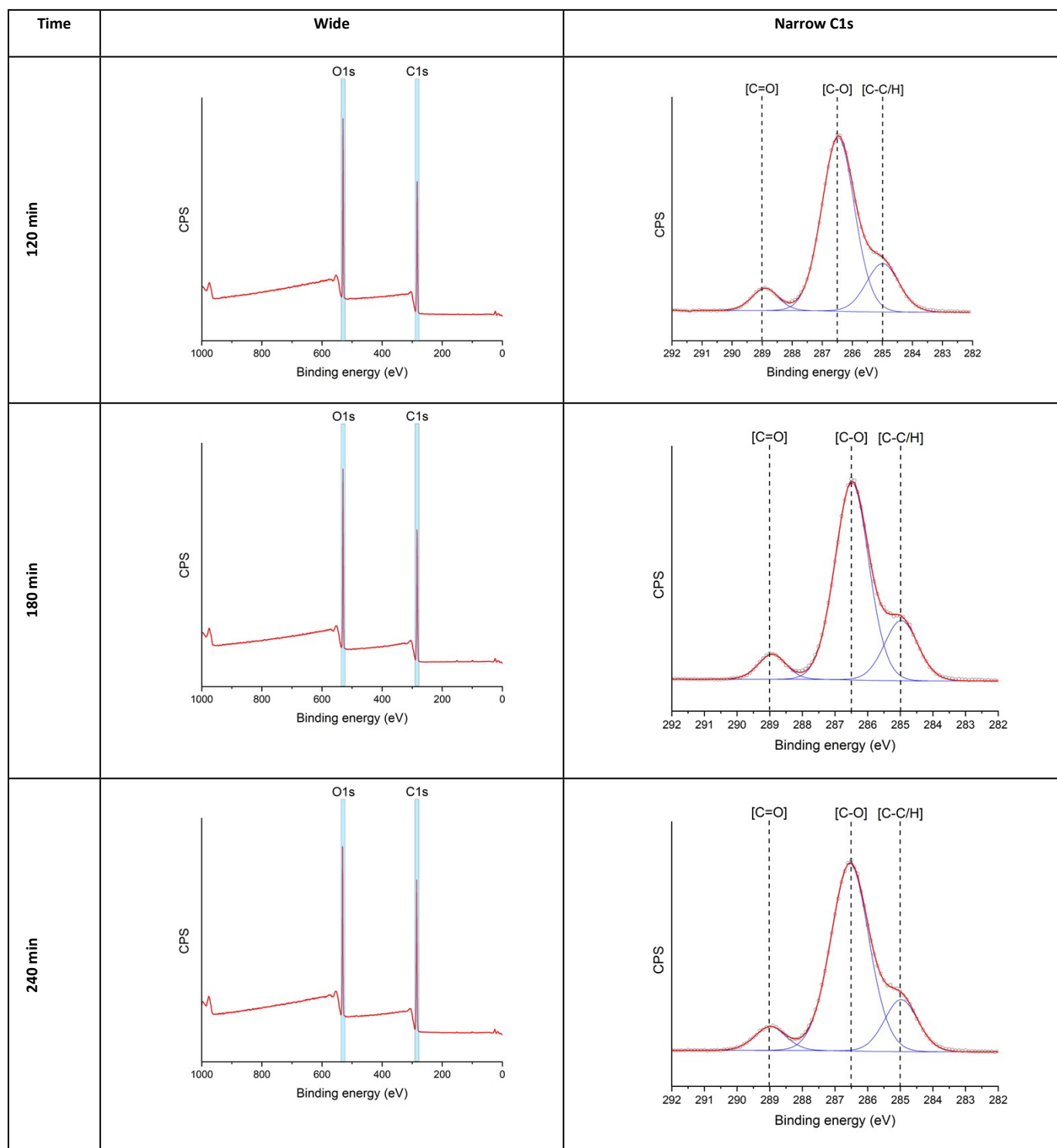


Table S10. XPS characterization of poly(MeOEGMA) brushes obtained by SI-PET-RAFT in no-flow conditions, EY photocatalyst, ratios between the peaks in XPS wide spectrum.

Time (min)	C1s	O1s
30	2.4	1.0
60	2.7	1.0
90	2.6	1.0
120	2.6	1.0
180	2.6	1.0
280	2.6	1.0
420	2.6	1.0

Table S11. XPS characterization of poly(MeOEGMA) brushes obtained by SI-PET-RAFT in flow conditions, EY photocatalyst, ratios between the peaks in XPS wide spectrum.

Time (min)	C1s	O1s
30	2.5	1.0
60	2.6	1.0
90	2.6	1.0
120	2.6	1.0
180	2.6	1.0
280	2.7	1.0
420	2.7	1.0

Table S12. XPS characterization of poly(MeOEGMA) brushes obtained by SI-PET-RAFT in no-flow conditions, R photocatalyst, ratios between the peaks in XPS wide spectrum.

Time (min)	C1s	O1s
30	2.7	1.0
60	2.6	1.0
180	2.6	1.0
220	2.6	1.0
420	2.6	1.0

Table S13. XPS characterization of poly(MeOEGMA) brushes obtained by SI-PET-RAFT in flow conditions, R photocatalyst, ratios between the peaks in XPS wide spectrum.

Time (min)	C1s	O1s
30	2.8	1.0
60	2.7	1.0
180	2.7	1.0
220	2.7	1.0
420	2.7	1.0

Table S14. XPS characterization of poly(MeOEGMA) brushes obtained by SI-PET-RAFT in no-flow conditions, Ph photocatalyst, ratios between the peaks in XPS wide spectrum.

Time (min)	C1s	O1s
30 min	2.7	1.0
60 min	2.6	1.0
120 min	2.7	1.0
180 min	2.6	1.0
240 min	2.6	1.0
420 min	2.6	1.0

Table S15. XPS characterization of poly(MeOEGMA) brushes obtained by SI-PET-RAFT in flow conditions, Ph photocatalyst, ratios between the peaks in XPS wide spectrum.

Time (min)	C1s	O1s
30	2.9	1.0
60	2.8	1.0
120	2.6	1.0
180	2.7	1.0
240	2.6	1.0
420	2.8	1.0

Table S16. XPS characterization of poly(MeOEGMA) brushes obtained by SI-PET-RAFT in no-flow conditions, EB photocatalyst, ratios between the peaks in XPS wide spectrum.

Time (min)	C1s	O1s
120 min	2.5	1.0
180 min	2.5	1.0
240 min	2.6	1.0

Table S17. XPS characterization of poly(MeOEGMA) brushes obtained by SI-PET-RAFT in flow conditions, EB photocatalyst, ratios between the peaks in XPS wide spectrum.

Time (min)	C1s	O1s
120	2.7	1.0
180	2.6	1.0
240	2.6	1.0

Table S18. XPS characterization of poly(MeOEGMA) brushes obtained by SI-PET-RAFT in no-flow conditions, EY photocatalyst, ratios between the peaks in XPS C1s narrow spectrum.

Time (min)	[C-C/H]	[C-O]	[C=O]
30 min	8.8	2.7	1.0
60 min	9.9	2.8	1.0
90 min	10.0	2.6	1.0
120 min	9.2	2.3	1.0
180 min	9.8	2.3	1.0
280 min	10.5	2.7	1.0
420 min	9.5	2.4	1.0

Table S19. XPS characterization of poly(MeOEGMA) brushes obtained by SI-PET-RAFT in flow conditions, EY photocatalyst, ratios between the peaks in XPS C1s narrow spectrum

Time (min)	[C-C/H]	[C-O]	[C=O]
30 min	9.6	3.2	1.0
60 min	9.5	2.6	1.0
90 min	9.4	2.6	1.0
120 min	9.4	3.7	1.0
180 min	10.1	2.5	1.0
280 min	10.2	3.0	1.0
420 min	10.1	2.5	1.0

Table S20. XPS characterization of poly(MeOEGMA) brushes obtained by SI-PET-RAFT in no-flow conditions, R photocatalyst, ratios between the peaks in XPS C1s narrow spectrum.

Time (min)	[C-C/H]	[C-O]	[C=O]
30	10.4	2.5	1.0
60	10.2	2.8	1.0
180	9.2	2.6	1.0
220	10.2	2.9	1.0
420	10.4	2.7	1.0

Table S21. XPS characterization of poly(MeOEGMA) brushes obtained by SI-PET-RAFT in flow conditions, R photocatalyst, ratios between the peaks in XPS C1s narrow spectrum.

Time (min)	[C-C/H]	[C-O]	[C=O]
30	9.7	3.2	1.0
60	10.6	3.3	1.0
180	9.5	3.1	1.0
220	9.6	2.8	1.0
420	9.3	2.9	1.0

Table S22. XPS characterization of poly(MeOEGMA) brushes obtained by SI-PET-RAFT in no-flow conditions, Ph photocatalyst, ratios between the peaks in XPS C1s narrow spectrum.

Time (min)	[C-C/H]	[C-O]	[C=O]
30	10.2	3.1	1.0
60	9.8	2.5	1.0
120	10.0	2.5	1.0
180	9.6	2.6	1.0
240	10.3	2.9	1.0
420	9.8	2.5	1.0

Table S23. XPS characterization of poly(MeOEGMA) brushes obtained by SI-PET-RAFT in flow conditions, Ph photocatalyst, ratios between the peaks in XPS C1s narrow spectrum.

Time (min)	[C-C/H]	[C-O]	[C=O]
30	9.6	3.7	1.0
60	9.6	2.6	1.0
120	10.3	2.5	1.0
180	9.6	2.9	1.0
240	9.9	2.9	1.0
420	9.3	3.4	1.0

Table S24. XPS characterization of poly(MeOEGMA) brushes obtained by SI-PET-RAFT in no-flow conditions, EB photocatalyst, ratios between the peaks in XPS C1s narrow spectrum.

Time (min)	[C-C/H]	[C-O]	[C=O]
120	9.6	3.7	1.0
180	9.6	2.6	1.0
240	10.3	2.5	1.0

Table S25. XPS characterization of poly(MeOEGMA) brushes obtained by SI-PET-RAFT in flow conditions, EB photocatalyst, ratios between the peaks in XPS C1s narrow spectrum.

Time (min)	[C-C/H]	[C-O]	[C=O]
120	9.7	2.7	1.0
180	9.6	2.9	1.0
240	9.6	2.3	1.0

Kinetics measurements

All samples were measured at least in quadruplicate.

Table S26. Evolution of dry thickness in time poly(MeOEGMA) brushes obtained by SI-PET-RAFT in no-flow conditions, EY photocatalyst.

Time (min)	Thickness (dry) (nm)	Error (nm)
30	17.6	1.3
60	25.5	0.1
90	28.1	1.3
120	25.5	1.3
150	31.5	0.4
180	29.4	0.6
220	30.4	0.9
240	28.5	1.1
280	31.4	1.6
420	32.8	0.3

Table S27. Evolution of dry thickness in time poly(MeOEGMA) brushes obtained by SI-PET-RAFT in flow conditions, EY photocatalyst.

Time (min)	Thickness (dry) (nm)	Error (nm)
30	21.4	0.5
60	46.1	4.9
90	50.7	4.5
120	64.3	2.7
150	64.8	11.5
180	69.2	6.6
220	85.6	7.8
240	88.1	3.9
280	93.2	4.4
420	124.5	9.3

Table S28. Evolution of dry thickness in time poly(MeOEGMA) brushes obtained by SI-PET-RAFT in no-flow conditions, R photocatalyst.

Time (min)	Thickness (dry) (nm)	Error (nm)
30	18.9	1.2
60	30.7	2.8
90	38.0	5.6
120	40.4	3.2
150	46.8	9.2
180	33.9	1.1
220	39.2	3.9
240	34.5	0.1
280	46.0	7.6
420	47.6	7.4

Table S29. Evolution of dry thickness in time poly(MeOEGMA) brushes obtained by SI-PET-RAFT in flow conditions, R photocatalyst.

Time (min)	Thickness (dry) (nm)	Error (nm)
30	21.0	0.4
60	18.3	1.2
90	41.1	5.5
120	61.5	18.4
150	72.0	26.4
180	94.9	13.9
220	97.8	9.2
240	146.7	20.6
280	152.0	23.4
420	239.3	24.8

Table S30. Evolution of dry thickness in time poly(MeOEGMA) brushes obtained by SI-PET-RAFT in no-flow conditions, Ph photocatalyst.

Time (min)	Thickness (dry) (nm)	Error (nm)
30	22.1	3.7
60	26.8	0.4
90	31.8	0.1
120	39.2	3.0
150	34.6	1.4
180	27.6	1.0
220	42.8	5.3
240	41.1	2.6
280	37.7	4.6
420	43.9	3.5

Table S31. Evolution of dry thickness in time poly(MeOEGMA) brushes obtained by SI-PET-RAFT in flow conditions, Ph photocatalyst.

Time (min)	Thickness (dry) (nm)	Error (nm)
30	25.5	0.4
60	42.5	2.0
90	59.0	7.3
120	66.0	2.0
150	95.1	12.8
180	150.1	28.3
220	146.2	11.8
240	170.8	19.6
280	184.5	13.6
420	256.2	10.0

Table S32. Evolution of dry thickness in time poly(MeOEGMA) brushes obtained by SI-PET-RAFT in no-flow conditions, EB photocatalyst.

Time (min)	Thickness (dry) (nm)	Error (nm)
30.0	9.2	1.4
60.0	30.5	4.6
90.0	35.3	6.1
120.0	53.0	11.3
150.0	54.5	11.9
180.0	64.6	9.4
220.0	71.6	14.4
240.0	68.1	8.8
280.0	93.3	22.0
420.0	134.5	15.1

Table S33. Evolution of dry thickness in time poly(MeOEGMA) brushes obtained by SI-PET-RAFT in flow conditions, EB photocatalyst.

Time (min)	Thickness (dry) (nm)	Error (nm)
30.0	9.2	1.4
60.0	30.5	4.6
90.0	35.3	6.1
120.0	53.0	11.3
150.0	54.5	11.9
180.0	64.6	9.4
220.0	71.6	14.4
240.0	68.1	8.8
280.0	93.3	22.0
420.0	134.5	15.1

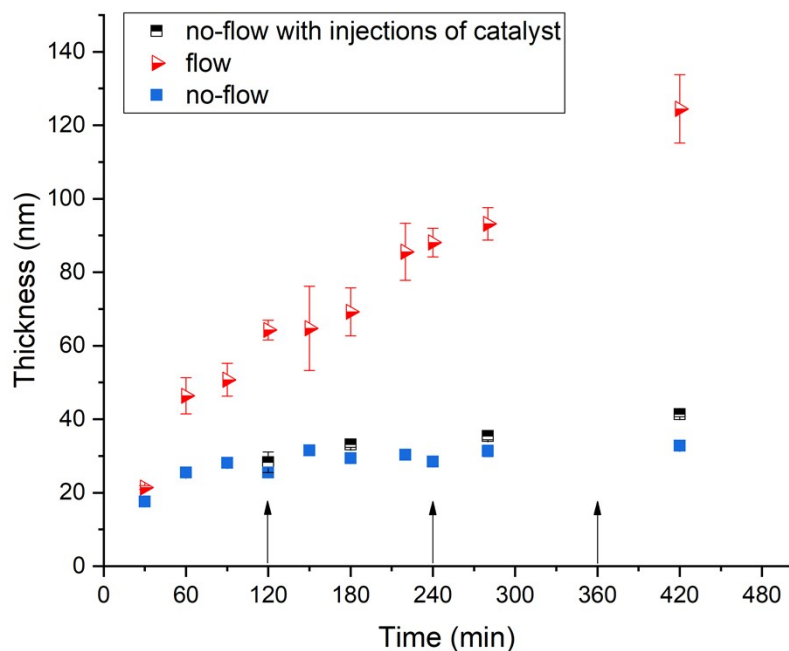


Figure S3. Dry thickness of poly(MeOEGMA) brushes as a function of the polymerization time, as determined by ellipsometry in flow, no-flow and no-flow with injection of 10 μ L of catalyst solution every 2 h (injections indicated by arrows). All samples were measured at least in duplicate.

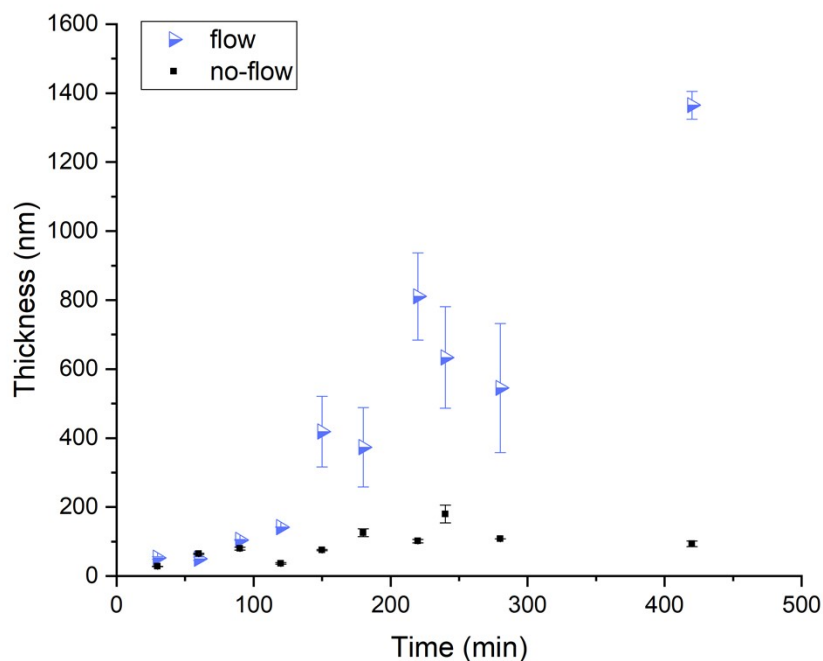


Figure S4. Dry thickness of poly(MeOEGMA) brushes as a function of the polymerization time, as determined by ellipsometry in flow and no-flow conditions using EY as photocatalysts in presence RAFT-agent in solution (free-RAFT). The molar ratio between M : EY : TEOA : free-RAFT agent 200 : 1 : 0.01 : 0.1. The 4-cyano-4-(phenylcarbonothioylthio)pentanoic acid was used as free (in solution) RAFT agent. All samples were measured at least in duplicate.

Table S34. Evolution of dry thickness in time poly(MeOEGMA) brushes obtained by SI-PET-RAFT in flow conditions, EY photocatalyst in the presence of RAFT agent.

Time (min)	Thickness (dry) (nm)	Error (nm)
30.0	52.8	3.4
60.0	50.3	5.2
90.0	104.8	1.7
120.0	141.9	0.6
150.0	418.8	102.1
180.0	373.6	114.8
220.0	810.5	125.9
240.0	633.7	147.5
280.0	545.3	187.0
420.0	1364.8	40.5

Table S35. Evolution of dry thickness in time poly(MeOEGMA) brushes obtained by SI-PET-RAFT in flow conditions, EY photocatalyst in the presence of RAFT agent.

Time (min)	Thickness (dry) (nm)	Error (nm)
30	28.3	0.4
60	64.3	2.0
90	79.7	3.9
120	36.7	2.5
150	75.2	1.7
180	125.5	11.5
220	101.4	4.9
240	180.0	25.9
280	107.7	0.1
420	93.8	8.2

SMFS measurements

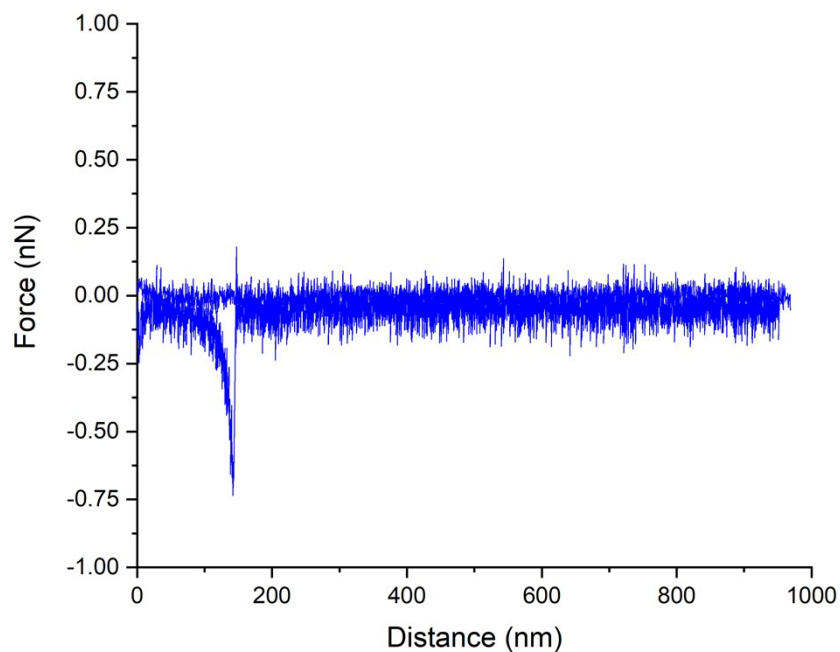


Figure S5. Representative retraction force curve measured on poly(MeOEGMA) brushes obtained by SI-PET-RAFT in flow conditions photocatalyst EY (polymerization time 5 min, dry thickness 11.7 nm) showing clear unfolding and rupture events.

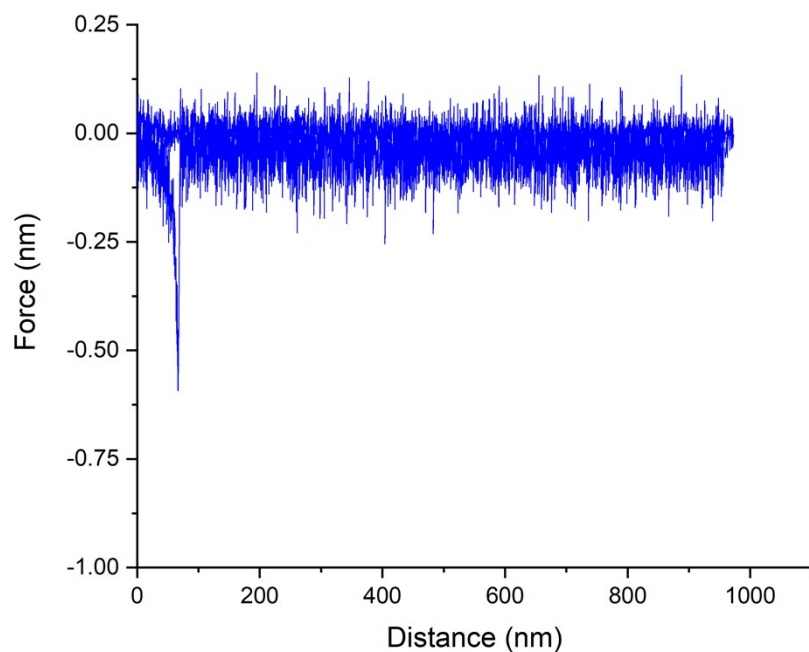


Figure S6. Representative retraction force curve measured on poly(MeOEGMA) brushes obtained by SI-PET-RAFT in flow conditions photocatalyst EY (polymerization time 5 min, dry thickness 15.7 nm) showing clear unfolding and rupture events.

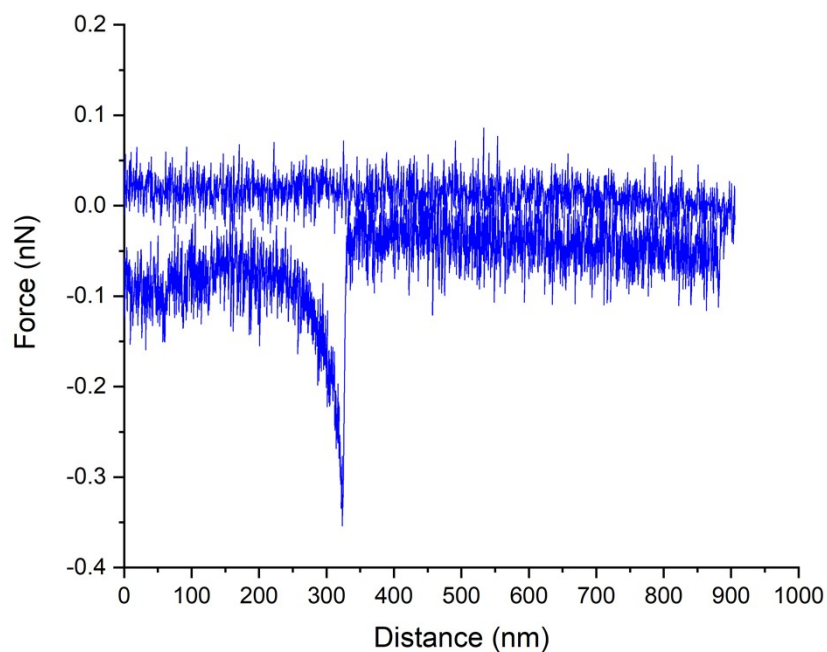


Figure S7. Representative retraction force curve measured on poly(MeOEGMA) brushes obtained by SI-PET-RAFT in flow conditions photocatalyst EY (polymerization time 60 min, dry thickness 50.3 nm) showing clear unfolding and rupture events.

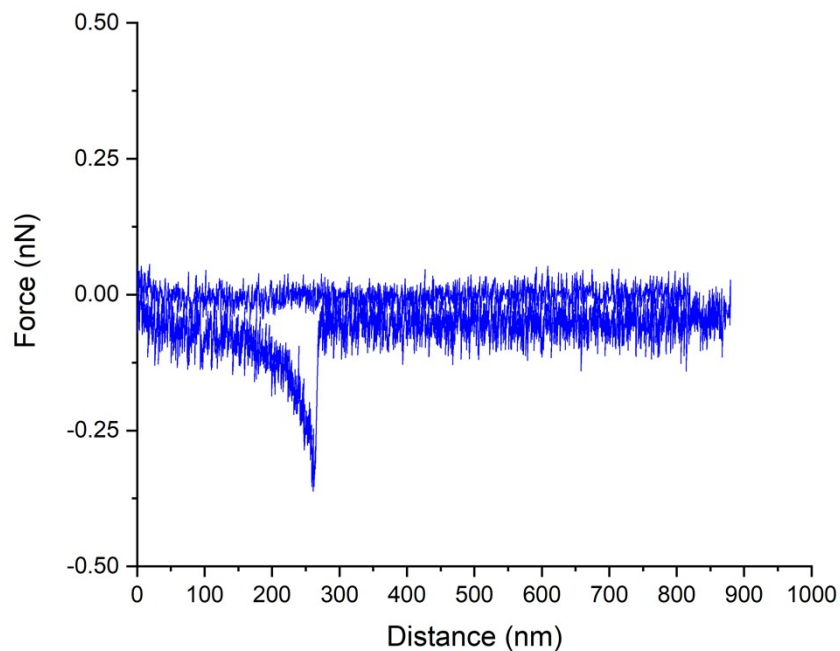


Figure S8. Representative retraction force curve measured on poly(MeOEGMA) brushes obtained by SI-PET-RAFT in no-flow conditions photocatalyst EY (polymerization time 120 min, dry thickness 36.7 nm) showing clear unfolding and rupture events.

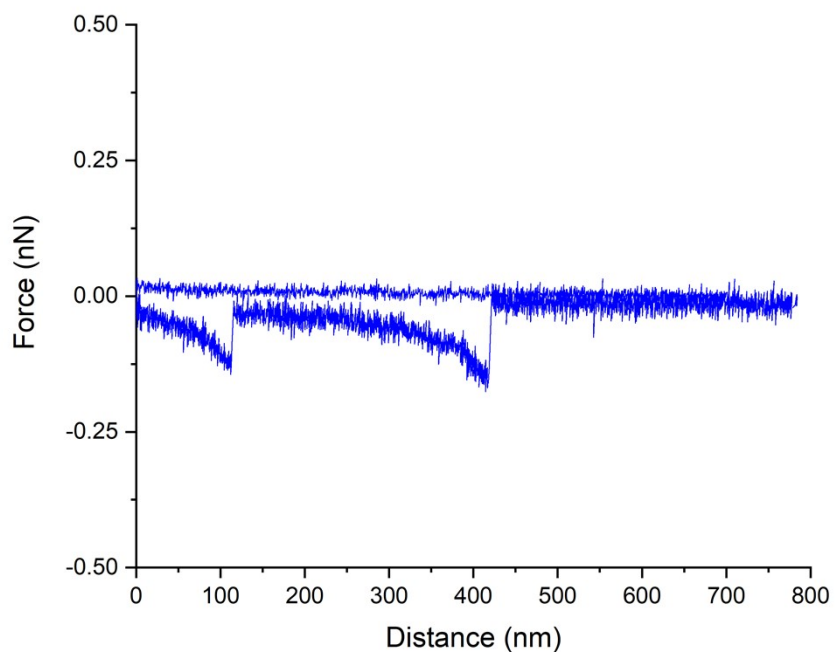


Figure S9. Representative retraction force curve measured on poly(MeOEGMA) brushes obtained by SI-PET-RAFT in flow conditions photocatalyst EY (polymerization time 60 min, dry thickness 50.3 nm) showing multiple rupture events.

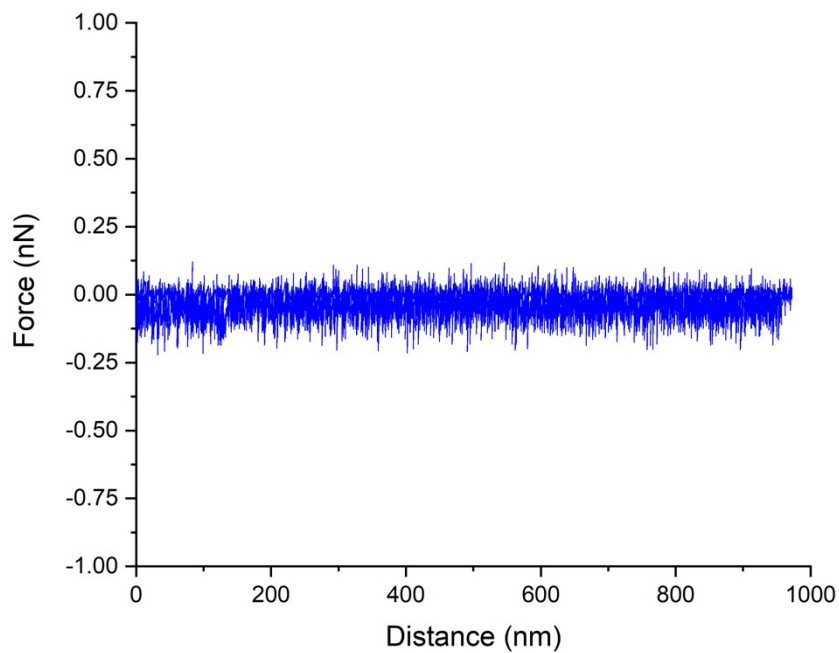


Figure S10. Representative retraction force curve measured on poly(MeOEGMA) brushes obtained by SI-PET-RAFT in flow conditions photocatalyst EY (polymerization time 5 min, dry thickness 11.2 nm) showing no rupture events.

Table S36. SMFS measurements results of poly(MeOEGMA) brushes obtained by SI-PET-RAFT in no-flow conditions, EY photocatalyst.

Time (min)	Thickness (dry) (nm)	Contour Length (nm)	Persist. Length (pm)	Residuals RMS (pN)	Fraction Rapture (%)	M_n (g·mol ⁻¹)	Grafting density σ (chains·nm ⁻²)	Monomer Units	Radius Gyration (nm)	Reduced Grafting Density Σ
5	7.3 ± 0.1	102 ± 5	124 ± 9	22.9 ± 0.6	0.81	112122 ± 5495	0.041	374	10	13
5	8.9 ± 0.3	72 ± 4	53 ± 4	83.0 ± 16.0	0.75	79471 ± 4396	0.071	264	8	16
5	9.2 ± 0.4	116 ± 6	43 ± 4	69.5 ± 13.8	0.58	127807 ± 6593	0.046	425	11	17
60	25.0 ± 1.2	146 ± 4	332 ± 18	63.1 ± 5.2	1.12	159931 ± 4396	0.099	535	12	45
120	36.7 ± 2.5	255 ± 18	23 ± 3	59.7 ± 5.0	0.3	280068 ± 19780	0.083	934	16	66

Table S37. SMFS measurements results of poly(MeOEGMA) brushes obtained by SI-PET-RAFT in flow conditions, EY photocatalyst.

Time (min)	Thickness (dry) (nm)	Contour Length (nm)	Persist. Length (pm)	Residuals RMS (pN)	Fraction Rapture (%)	M_n (g·mol ⁻¹)	Grafting density σ (chains·nm ⁻²)	Monomer Units	Radius Gyration (nm)	Reduced Grafting Density Σ
5	11.2 ± 3.1	120 ± 5	55 ± 4	65.5 ± 5.4	1.02	132258 ± 5495	0.054	440	20	124
5	15.7 ± 0.1	180 ± 13	73 ± 10	36.7 ± 6.4	0.62	197648 ± 14286	0.05	659	20	123
60	56.5 ± 0.7	423 ± 21	99 ± 14	16.2 ± 0.8	0.69	464879 ± 23077	0.094	1549	18	90
60	50.3 ± 5.2	340 ± 20	83 ± 7	35.9 ± 3.3	1.24	374023 ± 21978	0.085	1245	11	20
120	69.1 ± 3.3	412 ± 15	139 ± 9	12.7 ± 0.6	3.51	452491 ± 16484	0.096	1509	13	28

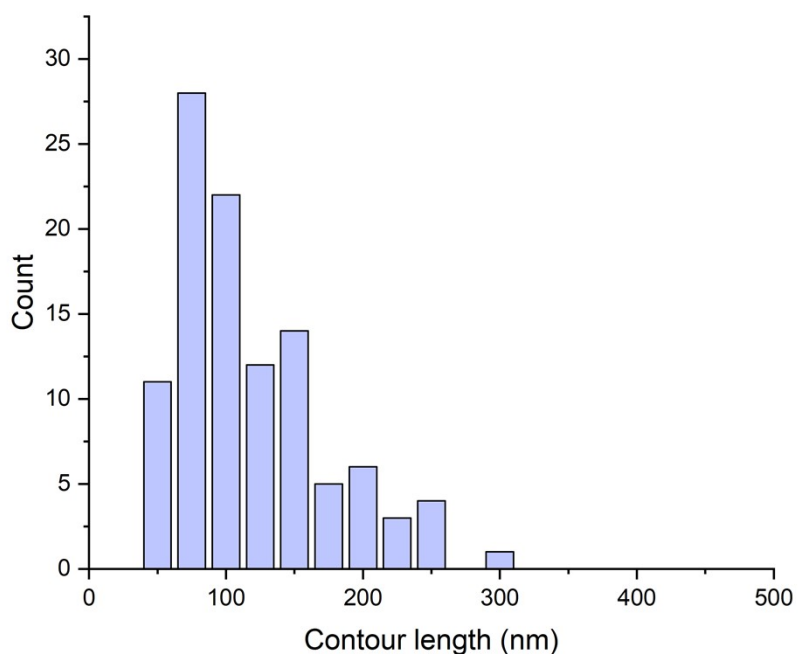


Figure S11. Distribution of contour lengths obtained from the fits model measured on thiol-terminated poly(MeOEGMA) brushes synthesized by SI-PET-RAFT in no-flow conditions, polymerization time 5 min, thickness 7.3 nm.

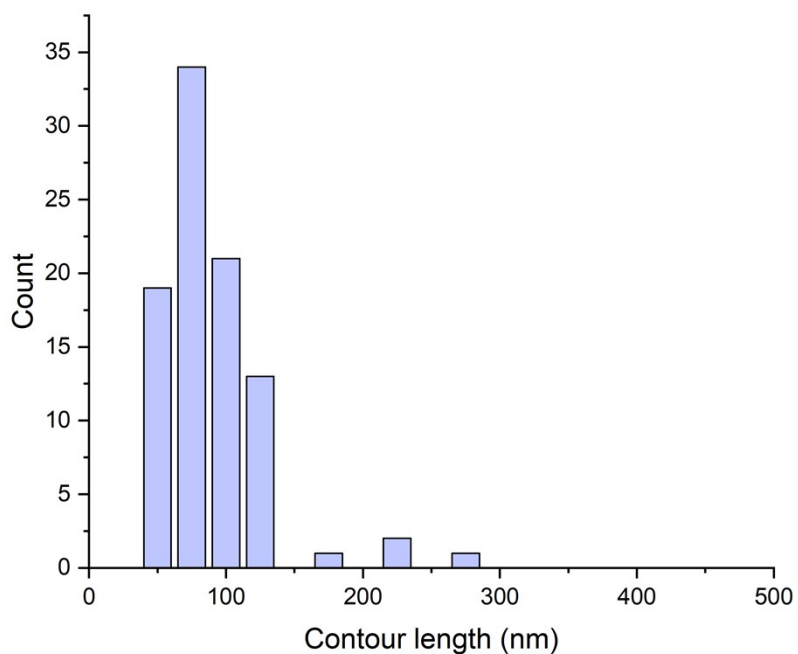


Figure S12. Distribution of contour lengths obtained from the fits to the wormlike-chain model as measured on thiol-terminated poly(MeOEGMA) brushes synthesized by SI-PET-RAFT in no-flow conditions, polymerization time 5 min, thickness 7.3 nm.

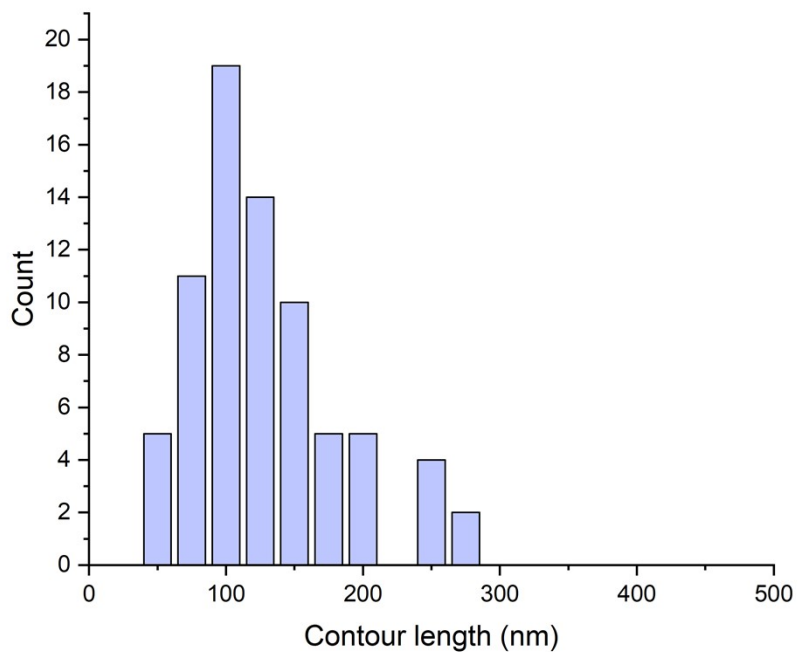


Figure 13. Distribution of contour lengths obtained from the fits to the wormlike-chain model as measured on thiol-terminated poly(MeOEGMA) brushes synthesized by SI-PET-RAFT in no-flow conditions, polymerization time 5 min, thickness 9.2 nm.

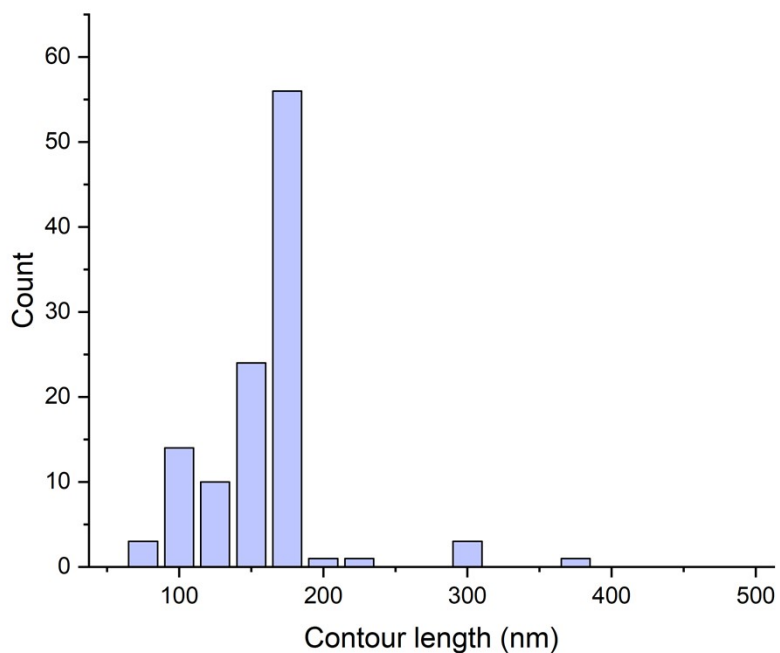


Figure S14. Distribution of contour lengths obtained from the fits to the wormlike-chain model as measured on thiol-terminated poly(MeOEGMA) brushes synthesized by SI-PET-RAFT in no flow conditions, polymerization time 60 min, thickness 25.0 nm.

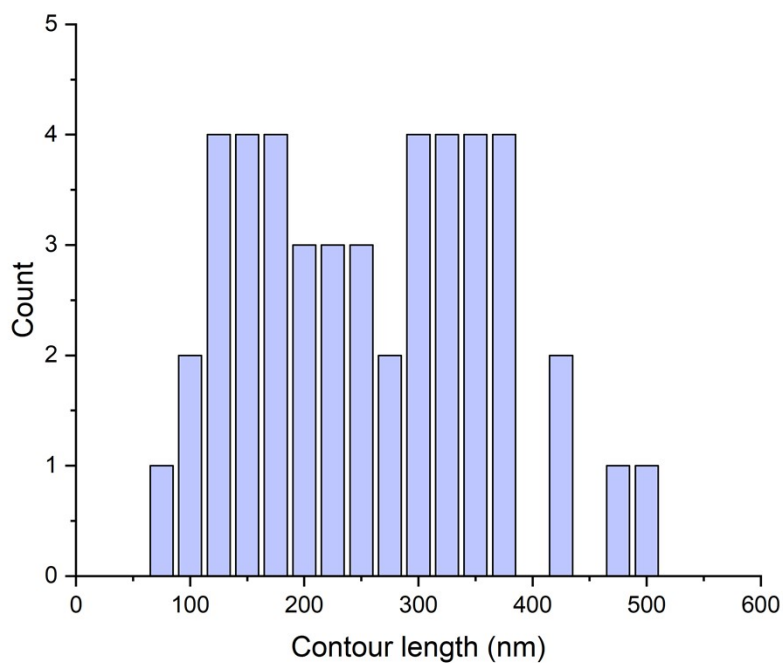


Figure S15. Distribution of contour lengths obtained from the fits to the wormlike-chain model as measured on thiol-terminated poly(MeOEGMA) brushes synthesized by SI-PET-RAFT in no flow conditions, polymerization time 120 min, thickness 36.7 nm.

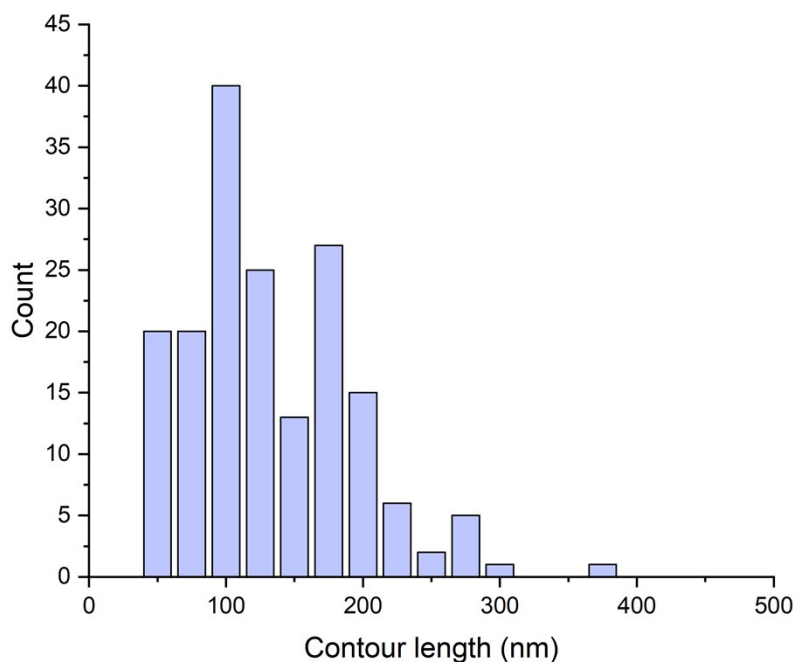


Figure S16. Distribution of contour lengths obtained from the fits to the wormlike-chain model as measured on thiol-terminated poly(MeOEGMA) brushes synthesized by SI-PET-RAFT in flow conditions, polymerization time 5 min, thickness 11.2 nm.

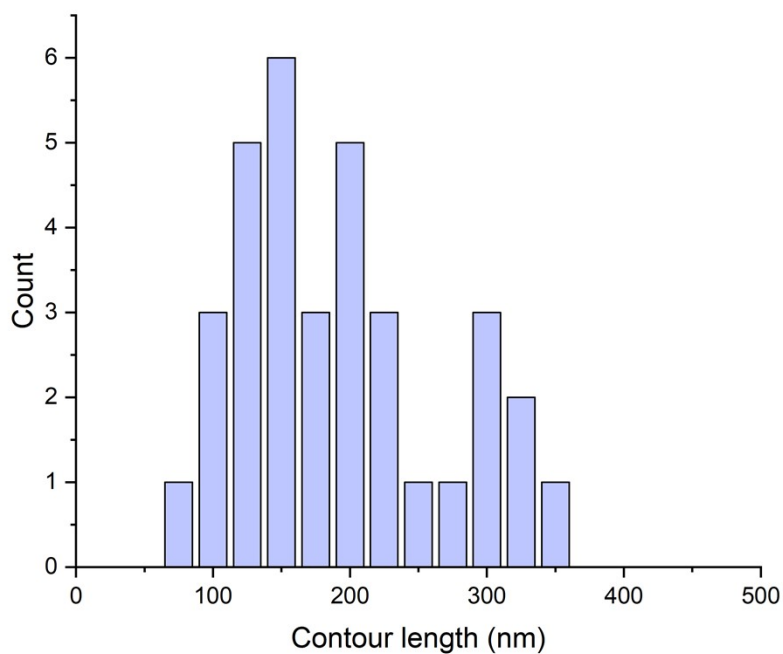


Figure S17. Distribution of contour lengths obtained from the fits to the wormlike-chain model as measured on thiol-terminated poly(MeOEGMA) brushes synthesized by SI-PET-RAFT in flow conditions, polymerization time 5 min, thickness 15.7 nm.

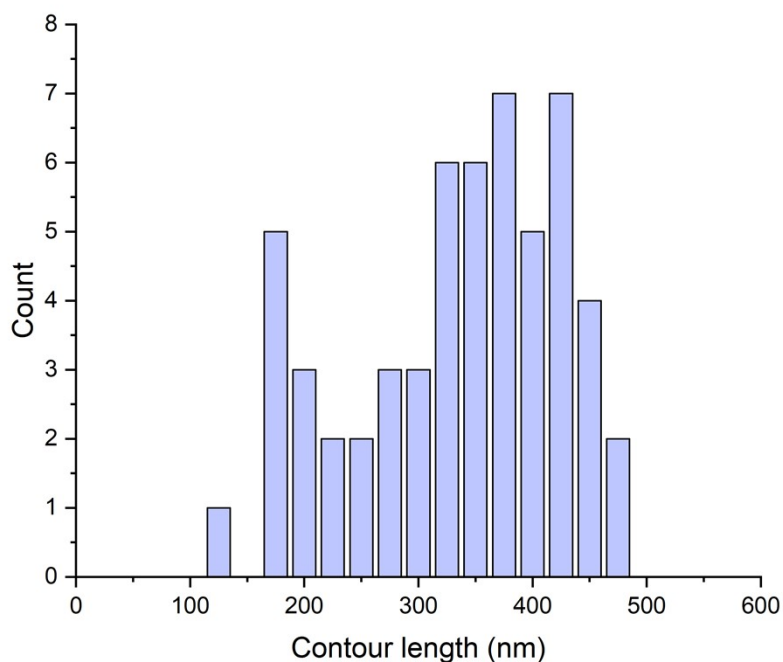


Figure S18. Distribution of contour lengths obtained from the fits to the wormlike-chain model as measured on thiol-terminated poly(MeOEGMA) brushes synthesized by SI-PET-RAFT in flow conditions, polymerization time 60 min, thickness 56.5 nm.

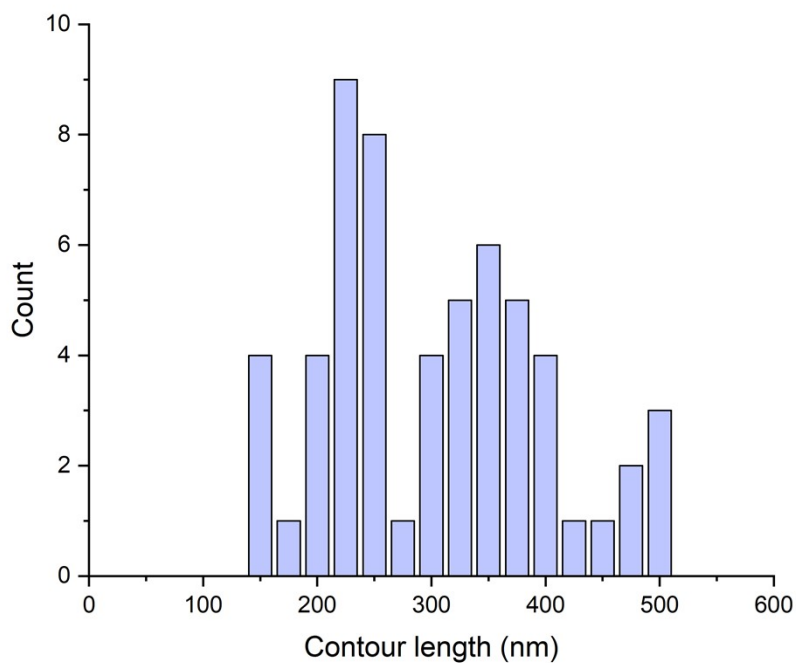


Figure S19. Distribution of contour lengths obtained from the fits to the wormlike-chain model as measured on thiol-terminated poly(MeOEGMA) brushes synthesized by SI-PET-RAFT in flow conditions, polymerization time 60 min, thickness 50.3 nm.

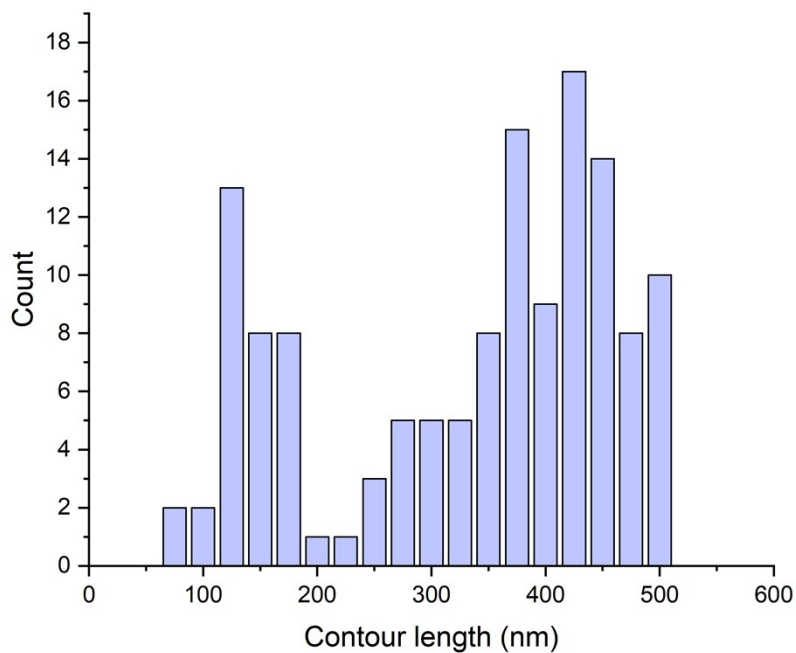


Figure S20. Distribution of contour lengths obtained from the fits to the wormlike-chain model as measured on thiol-terminated poly(MeOEGMA) brushes synthesized by SI-PET-RAFT in flow conditions, polymerization time 120 min, thickness 69.1 nm.

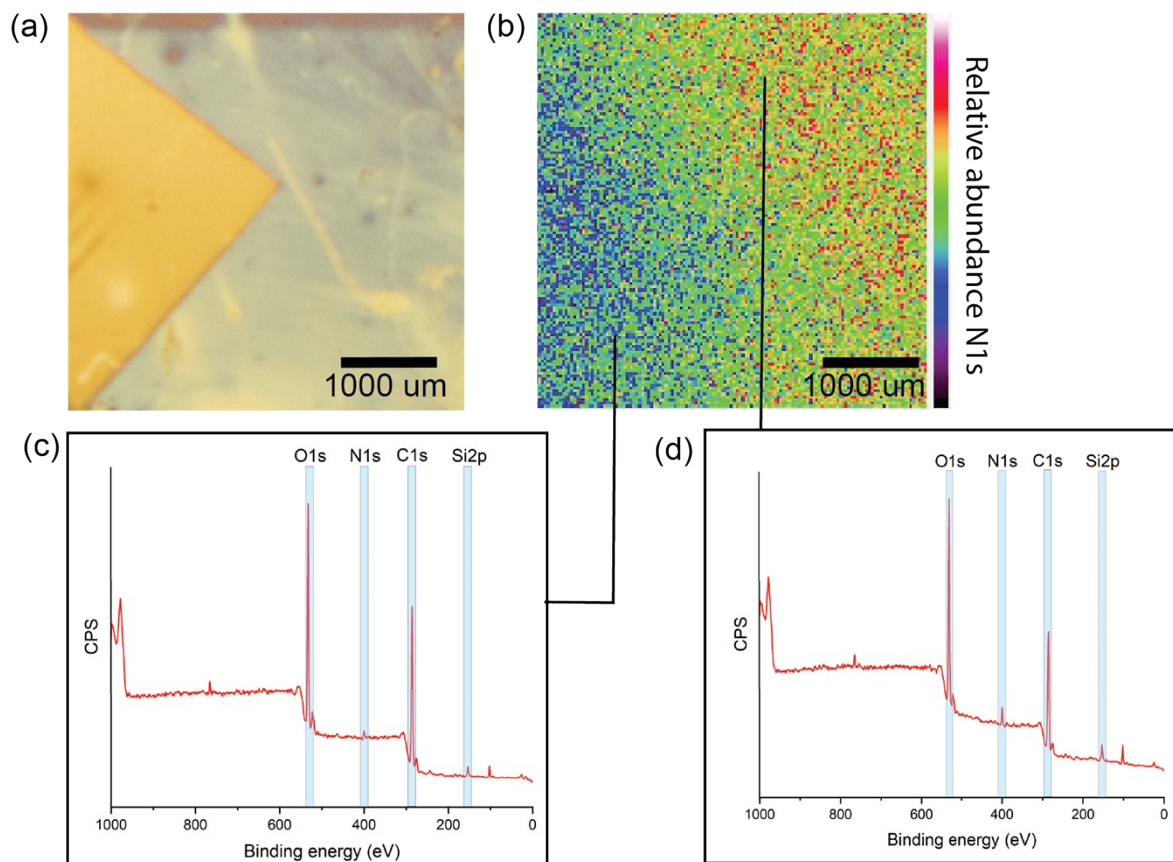


Figure S21. XPS mapping (a) optical image (b) intensity mapping of the nitrogen XPS signal at 400 eV, (c)(d) representative wide spectra XPS of different patterned regions.

References

- (1) Kuzmyn, A. R.; Nguyen, A. T.; Teunissen, L. W.; Zuilhof, H.; Baggerman, J. Antifouling Polymer Brushes via Oxygen-Tolerant Surface-Initiated PET-RAFT. *Langmuir* **2020**, *36* (16), 4439-4446.
- (2) Wang, Y.-M.; Kálosi, A.; Halahovets, Y.; Romanenko, I.; Slabý, J.; Homola, J.; Svoboda, J.; de los Santos Pereira, A.; Pop-Georgievski, O. Grafting Density and Antifouling Properties of Poly[N-(2-hydroxypropyl) Methacrylamide] Brushes Prepared by “Grafting to” and “Grafting from”. *Polym. Chem.* **2022**, *13* (25), 3815-3826.
- (3) Nečas, D.; Klapetek, P. Gwyddion: an Open-source Software for SPM Data Analysis. *Open Physics* **2012**, *10* (1), 181-188.